Journal of Inflammation Research

Dovepress
open access to scientific and medical research

Open Access Full Text Article

ORIGINAL RESEARCH

To Investigate the Mechanism of Qinpi Tongfeng Formula in Treating Acute Gouty Arthritis by UHPLC-Q-Orbitrap-MS, Network Pharmacology and Experimental Validation

Yihua Fan[1–3,*], Wei Liu[1,2,*], Yue Jin[1,2,*], Hang Lu[1,2], Chunliu Liu[1,2], Aihua Wang[1,2], Qingxiang Gu[1,2], Yuxiu Ka[1,2]

[1]Department of Rheumatism and Immunity, First Teaching Hospital of Tianjin University of Traditional Chinese Medicine, Tianjin, People's Republic of China; [2]National Clinical Research Center for Chinese Medicine Acupuncture and Moxibustion, Tianjin, People's Republic of China; [3]Department of Rheumatism and Immunity, Hospital of Chengdu University of Traditional Chinese Medicine, Chengdu, Sichuan Province, People's Republic of China

*These authors contributed equally to this work

Correspondence: Wei Liu, Email fengshiliuwei@163.com

Background: Acute gouty arthritis (AGA) is characterized by the accumulation of monosodium urate crystals within the joints, leading to inflammation and severe pain. Western medicine treatments have limitations in addressing this condition. Previous studies have shown the efficacy of Qinpi Tongfeng formula (QPTFF) in treating AGA, but further investigation is needed to understand its mechanism of action.

Methods: We used ultra-high-performance liquid chromatography tandem Q-Exactive Orbitrap high-resolution mass spectrometry (UHPLC-Q-Orbitrap-MS) to identify compounds in QPTFF. Target proteins regulated by these compounds were obtained from the Traditional Chinese Medicine Systems Pharmacology Database and Analysis Platform, Chemistry Database, and Swiss Target Prediction Database. AGA-related targets were searched and screened from various databases, including Genecards, PharmGKB, Drugbank, etc. Intersection targets of QPTFF and AGA were analyzed for protein–protein interaction networks, GO function enrichment, and KEGG pathway enrichment. We then verified QPTFF's mechanism of action using an AGA rat model, assessing pathological changes via H&E staining and target expression via ELISA, RT-qPCR, and Western blot.

Results: UHPLC-Q-Orbitrap-MS identified 207 compounds in QPTFF, with 55 selected through network pharmacology. Of 589 compound-regulated targets and 1204 AGA-related targets, 183 potential targets were implicated in QPTFF's treatment of AGA. Main target proteins included IL-1β, NFKBIA, IL-6, TNF, CXCL8, and MMP9, with the IL-17 signaling pathway primarily regulated by QPTFF. Experimental results showed that medium and high doses of QPTFF significantly reduced serum inflammatory factors and MMP-9 expression, and inhibited IL-17A, IL-6, IKK-β, and NF-κB p65 mRNA and protein expression in AGA rats compared to the model group.

Conclusion: Key targets of QPTFF include IL-1β, NFKBIA, IL-6, TNF-α, CXCL8, and MMP9. QPTFF effectively alleviates joint inflammation in AGA rats, with high doses demonstrating no liver or kidney toxicity. Its anti-inflammatory mechanism in treating AGA involves the IL-17A/NF-κB p65 signaling pathway.

Keywords: acute gouty arthritis, Qinpi Tongfeng formula, network pharmacology, UHPLC-Q-Orbitrap-MS, IL-17 signaling pathway

Introduction

As a metabolic rheumatic disorder, gout arises from the accumulation of urate in the joints, cartilage, and kidneys when serum uric acid increases to a certain extent due to abnormal purine metabolism in the human body.[1] The presence of acute gouty arthritis (AGA) is indicative of gout during its acute phase, which is characterized by sudden and severe joint pain, often recurrent.[2] Recurrent attacks of AGA can cause urate accumulation in joints, and kidney to cause joint

Received: 31 January 2024
Accepted: 17 May 2024
Published: 29 May 2024

destruction and chronic kidney disease and even renal failure, respectively.[3] Because gout is often accompanied by hyperuricemia, long-term hyperuricemia may cause an elevated risk of cardiovascular and cerebrovascular diseases.[4] The global prevalence of gout ranges from 1% to 6.8%. As modern living standards continue to improve, the prevalence of gout is steadily rising and affecting individuals at younger ages, largely attributed to shifts in dietary patterns and lifestyle habits.[5]

For the treatment of AGA, the American College of Rheumatology recommends drugs for inflammation and pain symptoms, which mainly include colchicine and non-steroidal anti-inflammatory drugs (NSAIDs).[6] While the administration of colchicine can promptly alleviate the patient's symptoms, varying levels of negative responses such as hepatic, renal, gastrointestinal impairment, and suppression of bone marrow may occur subsequent to treatment, and the disease is prone to rebound after drug withdrawal.[7,8] NSAIDs also have side effects such as gastrointestinal damage, liver and kidney damage and causing cardiovascular disease.[9] Hence, it is imperative to investigate a treatment option that ensures safety and efficacy while minimizing adverse reactions.

Traditional Chinese medicine (TCM) such as acupuncture and moxibustion, oral administration and external application of Chinese medicine, exerts a positive impact on AGA.[10–12] Compared with western medicine treatment alone, the external application of Chinese herbal medicine combined with western medicine treatment has better efficacy in the treatment of joint swelling and pain in patients with AGA.[13] Chinese herbal medicine can regulate macrophage autophagy through AMPKα/mTOR/ULK1 signaling pathway to alleviate MSU-induced arthritis.[14] Meanwhile, Chinese herbal medicine can promote M2 polarization of macrophages through PI3K/Akt signaling pathway, exert anti-inflammatory effects and improve joint symptoms of AGA rats.[15] The Qinpi Tongfeng formula (QPTFF) is optimized and improved from Qinpi powder in the ancient Chinese book *Taiping Shenghui recipe* (AD 992). QPTFF has been successfully utilized for over a decade at the First Affiliated Hospital of Tianjin University of TCM (TUTCM) as an effective compound in treating AGA. Prior research has established that QPTFF can relieve the symptoms of joint pain in AGA patients, which is equivalent to the efficacy of diclofenac sodium sustained-release tablets. At the same time, QPTFF can also improve the symptoms of joint swelling in AGA patients, reduce inflammatory markers and serum uric acid levels, and will not cause adverse effects on the liver and kidney function in AGA patients.[16] However, the primary compounds and mechanisms of QPTFF in treating AGA need to be further explored.

As an emerging research method, the application of network pharmacology has gained significant popularity in investigating single drugs and compounds of TCM in recent years.[17,18] Network pharmacology can predict biological informations such as the active components of TCM, TCM-related targets, TCM-related pathways, to investigate the potential mechanism of TCM at multiple levels, aligning with the distinctive attributes of TCM compounds that target multiple components and exert therapeutic effects. We used Ultra-high-performance liquid chromatography tandem Q-Exactive Orbitrap high-resolution mass spectrometry (UHPLC-Q-Orbitrap-MS) and network pharmacology methods to investigate the compounds and potential mechanisms of our formula. The mechanism of the anti-inflammatory effect of QPTFF in AGA based on IL-17A/NF-κB p65 signaling pathway was investigated through animal experiments, which provided a basis for the treatment of AGA with Chinese medicine. The study's research process is illustrated in Figure 1.

Materials and Methods

UHPLC-Q-Orbitrap-MS

Main Experimental Instruments

UHPLC-Q-Orbitrap-MS (Thermo, USA); Refrigerated centrifuges (Thermo, USA); KQ-300DV CNC ultrasonic cleaner (Kunshan Ultrasonic Instruments Co., Ltd., China); S0200-230V-EU vortex oscillator (Labnet, USA); N-1000 rotary evaporator (EYELA, Japan); Mill-Q-II ultra-pure water generator (Millipore, USA); FDU-2100 freeze dryer (EYELA, Japan).

Main Experimental Reagent

Formic acid was obtained from Tokyo Chemical Industry Co., Ltd. (Lot#: K3JHG.LS, purity ≥ 98%); Thermo Fisher Scientific Co., Ltd. was the source of chromatographic-grade methanol and acetonitrile.

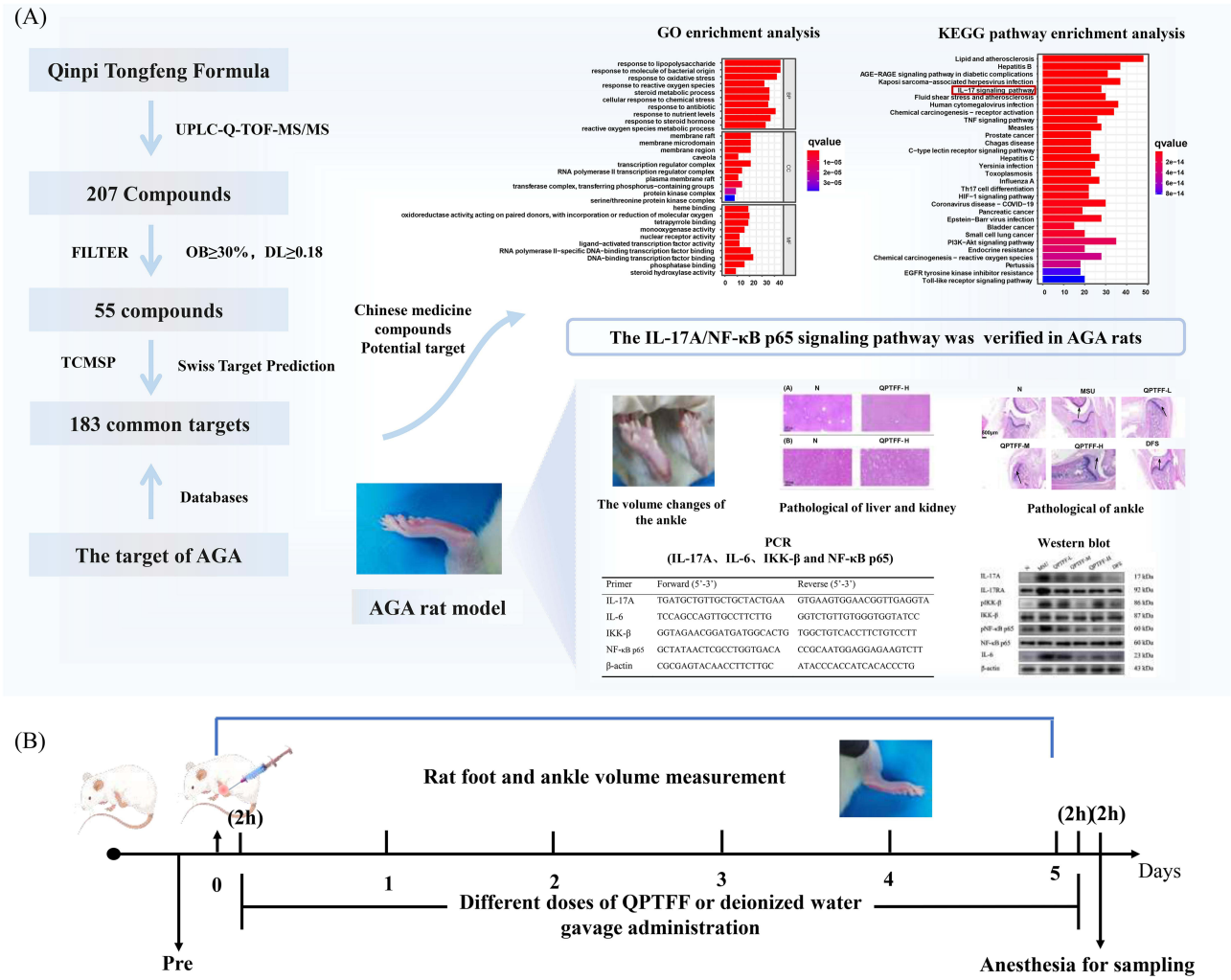

Figure 1 Flow chart of research scheme of Qinpi Tongfeng formula. (**A**) Flow chart of the entire experimental design; (**B**) Flow chart of animal experiment.

Preparation of Qinpi Tongfeng Formula Extract Solution

QPTFF was composed of Qinpi (*Cortex Fraxini*) 30 g, Tufuling (*Rhizoma Smilacis Glabrae*) 80 g, Huanglian (*Rhizoma Coptidis*) 10 g, Xixiancao (*Herba Siegesbeckiae*) 30 g, Bixie (*Rhizome Dioscoreae Hypoglaucae*) 30 g, Cheqianzi (*Semen Plantaginis*) 20 g, Weilingxian (*Radix Clematidis*) 20 g, and Fangfeng (*Radix Saposhnikoviae*) 10 g. The decoction pieces contained in QPTFF were purchased from the pharmacy of the First Teaching Hospital of Tianjin University of Traditional Chinese Medicine. These decoction pieces were identified by Dr Liming Wang of Tianjin University of Traditional Chinese Medicine. One dose of the aforementioned decoction pieces was placed in a round-bottomed flask, followed by the addition of 2000 mL of deionized water. After soaking for 30 min, the mixture was heated and boiled until approximately 200 mL of extractive solution was obtained. The extraction process was repeated twice, and subsequently, the extractive solutions were combined. After the extract was cooled naturally, we transferred it to a freeze-dryer for freeze-drying for 24 h by rotary evaporation concentration, and QPTFF extract powder was finally collected. We added QPTFF extract powder (1.00 g) with deionized water (10 mL) and dissolved by ultrasound for 30 min to obtain a stock solution. A total of 100 μL of stock solution was accurately measured, diluted with deionized water at a ratio of 10-fold, and passed through a membrane filter with a pore size of 0.22 μm to acquire a filtrate for subsequent analysis.

Chromatography and MS Parameters

The liquid chromatography was performed utilizing the UltiMate 3000 UHPLC system, which was linked to a column of ACQUITY UPLC HSS T3 column (2.1 mm × 100 mm, 1.8 μm). Mobile phase: 0.1% formic acid aqueous solution

(A)- acetonitrile (B); the flow rate was set 0.4 mL/min; elution procedure: 0 ~ 2.0 min; 1% B; 2 ~ 2.5 min, 1% ~ 10% B; 2.5 ~ 3.5 min, 10% ~ 20% B; 3.5 ~ 5.5 min, 20% ~ 30% B; 5.5 ~ 7.5 min, 30% ~ 46% B; 7.5 ~ 8.5 min, 46% ~ 100% B; 8.5 ~ 9.0 min, 100% B; 9.0 ~ 9.5 min, 100% ~ 1%B; 9.5 ~ 12.0 min, 1% B; adjust the temperature to 35 degree Celsius, while the injection volume was precisely measured at 2 microliters.

Mass Spectrum Condition

The mass spectrometric data were obtained in Thermo Fisher Q-Orbitrap MS (Q-Exative) system with high-energy electrospray ion source (HESI source), using Full-ms/dd-ms^2 scanning mode in both ionization polarities, namely positive and negative. The voltage applied to the source for positive ions was 3.5 kV, while for negative ions it was 2.8 kV. The capillary temperature during analysis was set at 320°C, and both the auxiliary gas and sheath gas (N_2) were maintained at temperatures of 350°C and a flow rate of 35 units, respectively. Auxiliary gas (N_2) was 10, S-lens level is 50 V, collision energy was set 20 V, 40 V, 60 V, scan range *m/z* 100 ~ 1500 Da.

Analysis of Network Pharmacology

Construction of Compounds Contained in Qinpi Tongfeng Formula and Their Targets

UHPLC-Q-Orbitrap-MS identified the screening of compounds of QPTFF. Oral Bioavailability (OB) and Drug likeness (DL) of them were obtained in the TCM Systems Pharmacology Database and Analysis Platform (TCMSP, https://old.tcmsp-e.com/tcmsp.php), and then screened (OB ≥ 30% and DL ≥ 0.18), and the targets corresponding to the compounds were obtained. If the compounds were not included in this platform, the OB values of the compounds of QPTFF were obtained through the Chemistry Database (http://www.organchem.csdb.cn/scdb/default.htm?nCount=196260370), and based on OB ≥ 30% for preliminary screening, the SMILES of the compounds were then downloaded using the PubChem database (https://pubchem.ncbi.nlm.nih.gov/), and we imported the SMILES into SwissADME database (http://www.swissadme.ch/) for prediction of drug-like properties,[19] opted components conforming to Lipinski's rule of 5.[20] Finally, the SMILES obtained were utilized in the Swiss Target Prediction database (http://www.swisstargetprediction.ch/) for drug target prediction and screened according to Probability > 0[21] to obtain the targets corresponding to the compounds of QPTFF.

Search for Genes Related to Acute Gouty Arthritis

We conducted a comprehensive search for AGA-related genes across multiple databases, including the Human Gene Database (Genecards, https://www.genecards.org/), Online Mendelian Inheritance in Man (OMIM, https://www.omim.org/), the pharmacogenomics knowledgebase database (PharmGKB, https://www.pharmgkb.org/), the Drugbank database (https://www.drugbank.ca/), DisGeNET database (https://www.disgenet.org/), the therapeutic target database (TTD, http://db.idrblab.net/ttd/), Comparative Toxicogenomics Database (CTD, http://ctdbase.org/) using the keywords "Acute gouty arthritis" or "Arthritis, Gouty". By merging the results from these databases and eliminating any duplicate target genes, we identified the relevant genes associated with AGA.

Predict Potential Targets of Qinpi Tongfeng Formula in Treating Acute Gouty Arthritis

We intersected the drug targets regulated by the compounds in QPTFF with the AGA-related targets to obtain common targets, ie potential targets of QPTFF in treating AGA. The Venn diagram of drug targets of QPTFF-AGA related targets was drawn.

Construct the "Chinese Medicine - Compounds - Potential Target" (CMCPT) Network

We utilized the Cytoscape 3.8.0 software to construct a network entitled "Chinese Medicine-Compounds-Potential Targets" that incorporates the potential targets of QPTFF for AGA treatment, along with their corresponding compounds, thereby facilitating visualization and analysis.

Construct the Protein–Protein Interaction (PPI) Networks and Screen Key Targets

Import potential QPTFF targets for AGA into STRING database (https://string-db.org/), selecting "Homo sapiens" as species and setting the minimum required interaction score to medium confidence (0.400), to obtain the PPI information and save it in "TSV" format, then "TSV" files were imported into Cytoscape 3.8.0 software to construct the PPI network.

The network's nodes were subjected to topological analysis using the CytoNCA plug-in. The topological parameters were Degree Centrality (DC), Betweenness Centrality (BC), Closeness Centrality (CC), Local Average Connectivity (LAC), and Eigenvector Centrality (EC). DC reflected frequency of node interaction with other nodes,[22] BC reflected the node's capacity to regulate the flow of information among other nodes, with greater BC indicating higher influence.[23] Compute DC for every node and eliminate nodes with DC ≥ the mean value as part of the initial screening process. Reconfigure a sub-network and employ the CytoNCA plug-in once more to compute the DC, BC, CC, LAC and EC values for the nodes within the sub-network. Subsequently, identify and filter out the nodes which are greater than the average value of each parameter to complete the second screening.

GO Functional and KEGG Pathway Enrichment Analyses

We utilized R 4.2.0 software along with the "org.Hs.eg.db" package to retrieve the IDs of the intersection targets, and then used "clusterProfiler". Subsequently, we employed various packages including "clusterProfiler" to conduct GO function enrichment analysis on them. The top 10 functional categories in Biological Process (BP), Cellular Component (CC) and Molecular function (MF) were selected. The KEGG enrichment analysis was performed on the intersection targets, and a demonstration was conducted by selecting the top 20 KEGG pathways.

Molecular Docking

The 2D structures of quercetin, eburicoic acid and polyporenic acid C were retrieved from the PubChem database (http://zinc.docking.org/). The 2D structures of the compounds were imported into Chem3D software to calculate the minimum free energy (.mol2) of the compounds. The 3D structures of the core targets were retrieved from the PDB protein structure database (http://www.rcsb.org/), and the water molecules and small molecular ligands (.PDB) were removed by PyMol software. The obtained macromolecular proteins and small molecular ligands were hydrotreated and converted into formats (.pdbqt and.gpf) by AutoDockTools software. Finally, the molecular docking was performed by AutoDock Vina program to calculate the minimum binding energy. The lower the binding energy, the stronger the binding force between the compound and the target. The binding energy was less than 0, indicating that the compound had a certain binding ability with the target. The binding energy was less than −5.0kJ/mol, indicating that the binding activity was good, and less than −7.0kJ/mol, indicating that the binding was stable.[24]

Experimental Verification

Experimental Animals

Six-week-old Sprague-Dawley male rats (SPF grade) weighing between 180 and 200 g were obtained from Beijing Huafukang Biotechnology Co., Ltd, animal license number: SCXK (Beijing) 2019–0008, housed at 20–25°C and 40–60% RH, and the experiments were carried out after 1 week of acclimatization. The Animal Ethics Committee of TUTCM granted approval for the animal experiment protocol (TCM-LAEC2021137).

Experimental Drug

The QPTFF dry paste powder made in the State Key Laboratory of Component TCM, TUTCM from the QPTFF decoction (see 2.1.3 for preparation method). Each dose of QPTFF could be converted into 13.99 g of dry paste powder. Diclofenac sodium (DFS) (0.1 g/tablet) was from Hunan Huana Pharmaceutical Co. (H20067776).

Experimental Instruments

Toe volume measurement instrument was from Jinan Benefit Technology Development Co., Ltd (YLS-7C); fully automatic dewatering machine was from Leica, Germany (ASP200S); paraffin sectioning machine was from Leica, Germany (RM2235); baking table was from Leica, Germany (HI1220); water bath was from Leica, Germany (HI1220); inverted phase contrast microscope was from Leica, Germany (DM3000); tabletop high-speed frozen centrifuge was from Beijing Beili Technology Co., Ltd (GTR16-2); fluorescence quantitative PCR instrument was from Thermo Fisher Scientific, USA (QuantStudio 1); electrophoresis instrument was from Beijing Liuyi Biotechnology Co., Ltd (DYY-6C); gel imager was from Beijing Saizhi Technology Co., Ltd (Champchemi 610 plus); spectrophotometer was from Shanghai Jeanqi Instrument Technology Co., Ltd (D8PCS).

Experimental Reagents

Monosodium urate (MSU) came from Shanghai Maclean Biochemical Technology Co., Ltd (U886060); IL-1βELISA kit was from Beijing Solabao Technology Co., Ltd (SEKR-0002); IL-8 ELISA kit was from Beijing Solaibao Technology Co., Ltd (SEKM-0071); IL-17A ELISA kit was from Wuhan Huamei Biological Engineering Co., Ltd (CSB-E07451r); IL-6 ELISA kit was from Wuhan PhD Biological Engineering Co., Ltd (EK0412); TNF-α ELISA kit was from Wuhan PhD Bioengineering Co., Ltd (EK0526); MMP-9 ELISA kit was from Wuhan PhD Bioengineering Co., Ltd (EK1463); Mouse Anti-βactin mAb (43 kDa) was from Beijing Zhongshan Jinqiao Biotechnology Co., Ltd (TA-09); IKK-β (87 kDa) antibody was from Wuhan PhD Biological Engineering Co., Ltd (PB9221); pIKK-β (86 kDa) antibody was from Bioworld (BS4101); NF-κB p65 (60 kDa) antibody was from Bioworld (BS3157); pNF-κB p65 (60 kDa) antibody was from Bioworld (BS4137); IL-6 (23 kDa) antibody was from Bioworld (BS6419); IL-17RA (92 kDa) antibody was from Beijing Bioss Company (bs-2606R); IL-17A (17 kDa) antibody was from Wuhan PhD Biological Engineering Co., Ltd (BA12416).

Establishment of AGA Rat Model and Experimental Grouping

Referring to the classical modeling method of Coderre et al[25] rats were anesthetized with a 1% sodium pentobarbital solution (5 mL/kg) administered intraperitoneally,[26] the selected injection orientation was the lateral posterior aspect of the right ankle joint followed by local disinfection. A 0.2 mL suspension of sodium urate crystals at a concentration of 50 mg/mL was administered into the ankle joint cavity using a 4.5-gauge needle, following the contralateral expansion of the joint capsule as the injection criterion. In contrast to the control group, the rats in the AGA model exhibited inflammation and edema in their right ankle joint, deepening of the color of the bottom of the foot in a reddish-purple color, slow walking, paw curling, and even hind limb prostration lameness, suggesting successful modeling.[27] After 7 days of acclimatization, divide 36 rats into normal control group (N), model group (MSU), Qinpi Tongfeng formula Low Dose Group (QPTFF-L), Qinpi Tongfeng formula Medium Dose Group (QPTFF-M), Qinpi Tongfeng formula High Dose Group (QPTFF-H), and Diclofenac Sodium Group (DFS) using the randomized zone group method. Six rats in each group, except for group N, were constructed as rat AGA model. 0.2 mL of saline was injected into the right ankle joint of group N. All rats were gavaged 2 h after modeling, and calculated a daily gavage dose of 10.5 mg/kg per rat for DFS group based on an equivalent dose ratio of 6.3 between rats and adults.[28] According to the ratio of 0.5:1:2 for low, medium and high doses, the gavage doses of QPTFF for rats in QPTFF-L, QPTFF-M, QPTFF-H groups were 0.74 g/kg, 1.47 g/kg and 2.94 g/kg, respectively. Rats in the group N and MSU group were gavaged with an equal volume of deionized water, and the remaining rats received daily gavage administration for a duration of 5 consecutive days.

Measurement of Foot and Ankle Volume in Rats

Right-sided ankle volumes were measured in all rats before (0 h), 2, 6, 12, 24, 48, 72 and 96 h after modeling using a pedicle volumetric instrument. The ankle volume of each rat was measured thrice the average value was utilized for statistical analysis.

Specimen Collection

Serum: After 2 h of gavage administration on day 5, rats were administered anesthesia through an intraperitoneal injection of a solution containing 1% sodium pentobarbital (5 mL/kg),[26] then collected whole blood from the abdominal aorta with a negative pressure blood collection tube and then centrifuged and stored the supernatant in a −80°C refrigerator. Ankle joint tissue: rats' skin was peeled off with the ankle joint as the center, and the upper and lower ends of the ankle joint were cut using a sterile scalpel, rinsed with physiological saline and then quickly placed in liquid nitrogen for preservation or fixed in 4% paraformaldehyde.

Histopathological Observation of the Ankle Joint

The ankle tissue was initially preserved in a solution containing 4% paraformaldehyde and subsequently subjected to decalcification using a 10% EDTA decalcifying solution. Successful decalcification was followed by torrefaction, transparency, wax immersion, embedding and sectioning. Hematoxylin and eosin staining were performed after dewaxing and hydration, and the ankle joint underwent histopathological alterations when examined using light microscopy.

Determination of Inflammatory Factors and MMP-9 in Rat Serum

The serum stored at −80°C was taken out, and relevant guidelines from the ELISA kit instructions were followed to assess IL-17A, IL-1β, IL-6, IL-8, TNF-α and MMP-9 levels in the serum.

mRNA Expression of Relevant Targets in Ankle Joint Tissues

We measured IL-17A, IL-6, IKK-β and NF-κB p65 mRNA expression in the test ankle tissue by Real-time PCR. Each sample was repeated 3 times. Total RNA was first extracted from 50 mg AGA rat ankle tissue samples containing 1 mL Trizol lysate, and the RNA purity and concentration were detected by spectrophotometer, where the purity was judged by the ratio of OD260/OD280. Two μg of total RNA was taken for reverse transcription, using reverse transcription reaction conditions (37°C, 15 min; 85°C, 5 s). Then the cDNA obtained from the completed reverse transcription was diluted 10 times and stored at −80°C for backup. Prepare 50 μL qRT-PCR system, place the octet in Step One Plus TM Real-Time PCR System, with 1 cycle of pre-denature (95°C,10 min), 40 cycles of denature and anneal/extend. Calculate gene expression levels with the $2^{-\Delta\Delta Ct}$ method. The primer sequences of the gene were synthesized by Shanghai Biotech Bioengineering Co., Ltd (Table 1).

Detection of Relevant Protein Expression in Ankle Joint Tissues Using Western Blot

IL-17A, IL-17RA, IKK-β, pIKK-β, NF-κB p65, pNF-κB p65 and IL-6 protein levels were measured with Western blot. Fifty milligrams of tissue from the ankle joint were collected and mixed with 500 μL of RIPA lysate, which contained a protease inhibitor (1% PMSF) and a phosphatase inhibitor (1%). The ankle tissue was subsequently subjected to ice-cold lysis for a duration of 30 min, followed by centrifugation at 13,000 g for 13 min at a temperature of 4°C. Subsequently, the supernatant was carefully transferred into a centrifuge tube with a capacity of 1.5 mL. Protein concentrations were detected by the BCA method. Based on the protein concentration values, the concentration of each group of proteins was diluted to 4.34 μg/μL with cell lysate, and then 5 × loading buffer was added at a ratio of 4:1 to make a protein loading solution concentration of 3.47 μg/μL. The proteins were denatured by cooking in a 95°C water bath for 10 min, and the samples were dispensed and stored in a −20°C refrigerator. The electrophoretic technique was employed to separate the proteins, followed by their subsequent transfer onto PVDF membranes and then it was closed in 5% BSA solution for 2 h. Dilute the primary antibody (1:500 for IKK-β antibody and 1:1000 for the rest of the primary antibody) with reference to the dilution ratio recommended in the instruction manual and previous experimental experience, and wash the membrane with TBST three times at room temperature. Then, secondary antibody was added, where the dilution ratio of secondary antibody was 1:5000, and incubated at 55 rpm for 90 min at room temperature; Use TBST was to wash the membrane 3 times. Observe protein bands according to the ECL chemiluminescence detection method, and use Image-J software to analyze them and calculate the grayscale values.

Observation of Rat Liver and Kidney Tissues by H&E Staining

In order to investigate whether QPTFF high dose would cause liver and kidney damage to normal blank rats, randomly divide 6 male rats into N group and 3 rats each in QPTFF-H group after 7 days of adaptive feeding, and no rat AGA model was constructed for both groups, and QPTFF-H group was administered continuously by gavage for 5 days (the administered dose was 2.94 g/kg). The rats were executed after administration on day 5, and the livers and kidneys of both groups underwent PBS washing, followed by fixation using 4% paraformaldehyde and subsequent preservation for the generation of pathological sections, which were stained with H&E and observed under light microscopy for specific morphology.

Table 1 qRT-PCR Primer Design

Primer	Forward (5'-3')	Reverse (5'-3')
IL-17A	TGATGCTGTTGCTGCTACTGAA	GTGAAGTGGAACGGTTGAGGTA
IL-6	TCCAGCCAGTTGCCTTCTTG	GGTCTGTTGTGGGTGGTATCC
IKK-β	GGTAGAACGGATGATGGCACTG	TGGCTGTCACCTTCTGTCCTT
NF-κB p65	GCTATAACTCGCCTGGTGACA	CCGCAATGGAGGAGAAGTCTT
β-actin	CGCGAGTACAACCTTCTTGC	ATACCCACCATCACACCCTG

Statistical Methods

The SPSS 22.0 was employed to complete a thorough statistical analysis of the data obtained, with the results presented as (Mean ± SD), and repeated measures ANOVA was used for multiple time point comparisons if the measures satisfied normality and chi-squaredness. Use One-way ANOVA to compare groups at a single time point, and select LSD test to compare groups, and a significance level of $P < 0.05$ to determine statistically significant distinction. Perform the plotting of all data with GraphPad Prism 8.

Outcomes

Compounds in Qinpi Tongfeng Formula

We analyzed the extracts of QPTFF by UHPLC-Q-Orbitrap-MS to obtain the total ion flow diagrams in positive and negative ion modes (Figure 2). Combined with the literature,[29–35] based on the chromatographic information and mass

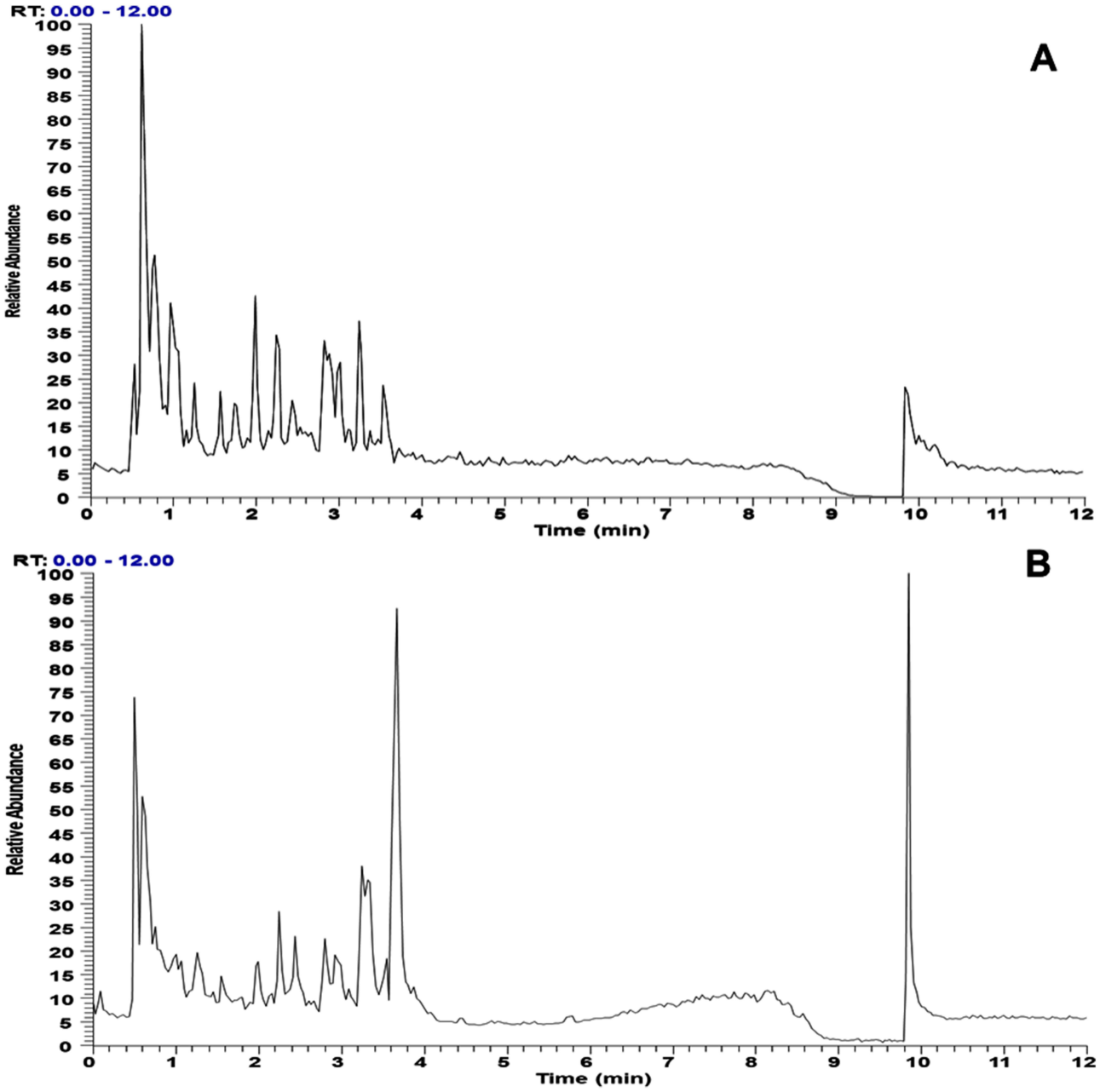

Figure 2 Total ion flow diagram of extract of Qinpi Tongfeng formula under positive (**A**) and negative ion (**B**) detection modes.

spectrometry information of the compounds, Qinpi (*Cortex Fraxini*) contained 30 compounds, Tufuling (*Rhizoma Smilacis Glabrae*) contained 36 compounds, Huanglian (*Rhizoma Coptidis*) contained 33 compounds, Bixie (*Rhizome Dioscoreae Hypoglaucae*) contained 10 compounds, Xixiancao (*Herba Siegesbeckiae*) contained 24 compounds, Cheqianzi (*Semen Plantaginis*) contained 47 compounds, Weilingxian (*Radix Clematidis*) contained 25 compounds, and Fangfeng (*Radix Saposhnikoviae*) contained 31 compounds, for a total of 236 compounds, and 207 compounds were finally obtained by removing the duplicates (Supplementary material Table S1).

Compounds of Qinpi Tongfeng Formula and QPTFF-Related Targets

With the criteria of OB ≥30% and DL ≥0.18, Qinpi (*Cortex Fraxini*) contained 4 compounds, Huanglian (*Rhizoma Coptidis*) contained 8 compounds; Fangfeng (*Radix Saposhnikoviae*) contained 8 compounds; Cheqianzi (*Semen Plantaginis*) contained 11 compounds; Tufuling (*Rhizoma Smilacis Glabrae*) contained 17 compounds; Bixie (*Rhizome Dioscoreae Hypoglaucae*) contained 2 compounds; Weilingxian (*Radix Clematidis*) contained 5 compounds; and Xixiancao (*Herba Siegesbeckiae*) contained 4 compounds. After removing the duplicate compounds, 55 compounds of QPTFF were obtained. Totally, 1659 compound-related targets were searched on the TCMSP and Swiss Target Prediction platforms, and 589 drug targets of QPTFF were obtained after deleting duplicate targets. Table 2 shows the compounds contained in QPTFF and the number of targets regulated.

Table 2 Compounds and the Number of Regulatory Targets of Qinpi Tongfeng Formula

Number	Source	Compounds	Number of Targets
1	Cheqianzi(*Semen Plantaginis*), Xixiancao(*Herba Siegesbeckiae*), Tufuling(*Rhizoma Smilacis Glabrae*)	quercetin	133
2	Tufuling(*Rhizoma Smilacis Glabrae*)	polyporenic acid C	100
3	Fangfeng(*Radix Saposhnikoviae*)	decursin	99
4	Huanglian(*Rhizoma Coptidis*)	moupinamide	99
5	Fangfeng(*Radix Saposhnikoviae*)	decursinol angelate	96
6	Tufuling(*Rhizoma Smilacis Glabrae*)	eburicoic acid	91
7	Tufuling(*Rhizoma Smilacis Glabrae*)	16α-hydroxytrametenolic acid	83
8	Tufuling(*Rhizoma Smilacis Glabrae*)	poricoic acid G	73
9	Tufuling(*Rhizoma Smilacis Glabrae*)	dehydroeburicoic acid	71
10	Tufuling(*Rhizoma Smilacis Glabrae*)	dehydropachymic acid	60
11	Cheqianzi(*Semen Plantaginis*)	ixoroside	56
12	Cheqianzi(*Semen Plantaginis*)	luteolin	53
13	Qinpi(*Cortex Fraxini*)	caffeic acid	52
14	Tufuling(*Rhizoma Smilacis Glabrae*)	pachymic acid	44
15	Cheqianzi(*Semen Plantaginis*)	campenoside	38
16	Tufuling(*Rhizoma Smilacis Glabrae*)	poricoic acid BM	38
17	Xixiancao(*Herba Siegesbeckiae*)	monopalmitin	35
18	Cheqianzi(*Semen Plantaginis*)	baicalein	34
19	Weilingxian(*Radix Clematidis*)	nobiletin	34
20	Cheqianzi(*Semen Plantaginis*), Xixiancao(*Herba Siegesbeckiae*)	stigmasterol	27
21	Weilingxian(*Radix Clematidis*)	clematomandshurica saponin B	25
22	Huanglian(*Rhizoma Coptidis*)	berberrubine	22
23	Cheqianzi(*Semen Plantaginis*)	monomelittoside	20
24	Huanglian(*Rhizoma Coptidis*)	berlambine	18
25	Bixie(*Rhizome Dioscoreae Hypoglaucae*)	ginsenoside Rd	18
26	Fangfeng(*Radix Saposhnikoviae*)	marmesin	18

(*Continued*)

Table 2 (Continued).

Number	Source	Compounds	Number of Targets
27	Fangfeng(*Radix Saposhnikoviae*)	nodakenetin	18
28	Huanglian(*Rhizoma Coptidis*)	palmatine	17
29	Huanglian(*Rhizoma Coptidis*)	berberine	16
30	Qinpi(*Cortex Fraxini*)	acetoxypinoresinol	15
31	Tufuling(*Rhizoma Smilacis Glabrae*), Bixie(*Rhizome Dioscoreae Hypoglaucae*)	diosgenin	14
32	Cheqianzi(*Semen Plantaginis*)	hispidulin	14
33	Cheqianzi(*Semen Plantaginis*)	hypolaetin	11
34	Weilingxian(*Radix Clematidis*)	liquiritigenin	11
35	Huanglian(*Rhizoma Coptidis*)	epiberberine	10
36	Qinpi(*Cortex Fraxini*)	medioresinol	10
37	Tufuling(*Rhizoma Smilacis Glabrae*)	taxifolin	10
38	Huanglian(*Rhizoma Coptidis*)	coptisine	8
39	Fangfeng(*Radix Saposhnikoviae*)	anomalin	7
40	Fangfeng(*Radix Saposhnikoviae*)	α-pinene	7
41	Huanglian(*Rhizoma Coptidis*)	worenine	6
42	Cheqianzi(*Semen Plantaginis*)	6-hydroxyluteolin	5
43	Tufuling(*Rhizoma Smilacis Glabrae*)	astilbin	5
44	Tufuling(*Rhizoma Smilacis Glabrae*)	cis-Dihydroquercetin	5
45	Weilingxian(*Radix Clematidis*)	embinin	5
46	Qinpi(*Cortex Fraxini*)	fraxin	5
47	Tufuling(*Rhizoma Smilacis Glabrae*)	isoastilbin	5
48	Fangfeng(*Radix Saposhnikoviae*)	phelloptorin	5
49	Tufuling(*Rhizoma Smilacis Glabrae*)	(-)-taxifolin	3
50	Fangfeng(*Radix Saposhnikoviae*)	pentanol	3
51	Cheqianzi(*Semen Plantaginis*)	baicalin	2
52	Xixiancao(*Herba Siegesbeckiae*)	darutigenol	2
53	Tufuling(*Rhizoma Smilacis Glabrae*)	β-sitosterol	1
54	Weilingxian(*Radix Clematidis*)	linarin	1
55	Tufuling(*Rhizoma Smilacis Glabrae*)	trametenolic acid	1

Collection of AGA-Related Genes and Potential Targets Prediction

In total, we obtained 1204 AGA-related targets by searching in Genecards, OMIM, PharmGKB, Drugbank, DisGeNET, TTD and CTD databases. We intersected the QPTFF-regulated targets with the AGA-related targets and gained 183 intersected targets that were potential QPTFF-targets in treating AGA (Figure 3).

Construct the "Chinese Medicine - Compounds - Potential Target" Network

We used Cytoscape 3.8.0 to construct the "Chinese medicine - Compounds - Potential target" network (Figure 4). The graph had a total of 240 nodes (48 compounds, 183 potential targets, 8 drug names, and 1 multidrug). The green square nodes represented potential targets for the regulation of QPTFF, the blue square nodes represented the Chinese herbs in QPTFF, and the yellow diamond nodes represented the compounds in QPTFF. The relationship between nodes suggested a targeted association between drug compounds and potential targets, with larger node degrees and larger node area corresponding to greater significance. Quercetin, eburicoic acid and polyporenic acid C were the top three compounds in Degree value. Among them, quercetin acted on 77 potential targets, which came from Cheqianzi (*Semen Plantaginis*), Tufuling (*Rhizoma Smilacis Glabrae*) and Xixiancao (*Herba Siegesbeckiae*); eburicoic acid was found to act on 37 potential targets from Tufuling (*Rhizoma Smilacis Glabrae*); polyporenic acid C was found to act on 35 potential targets and was derived from Tufuling (*Rhizoma Smilacis Glabrae*).

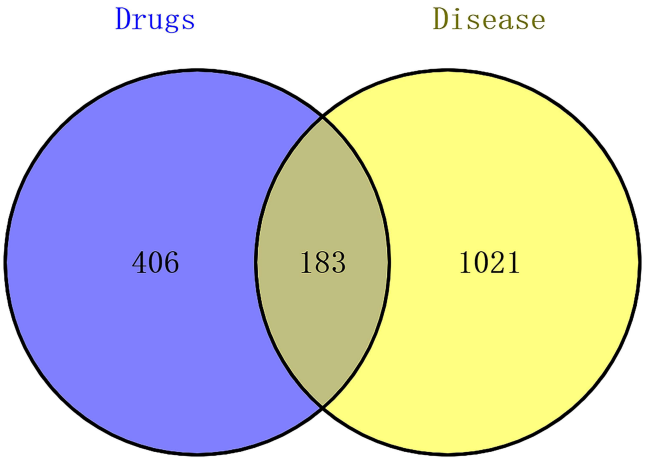

Figure 3 Venn diagram of Qinpi Tongfeng formula-related targets and AGA-related targets.

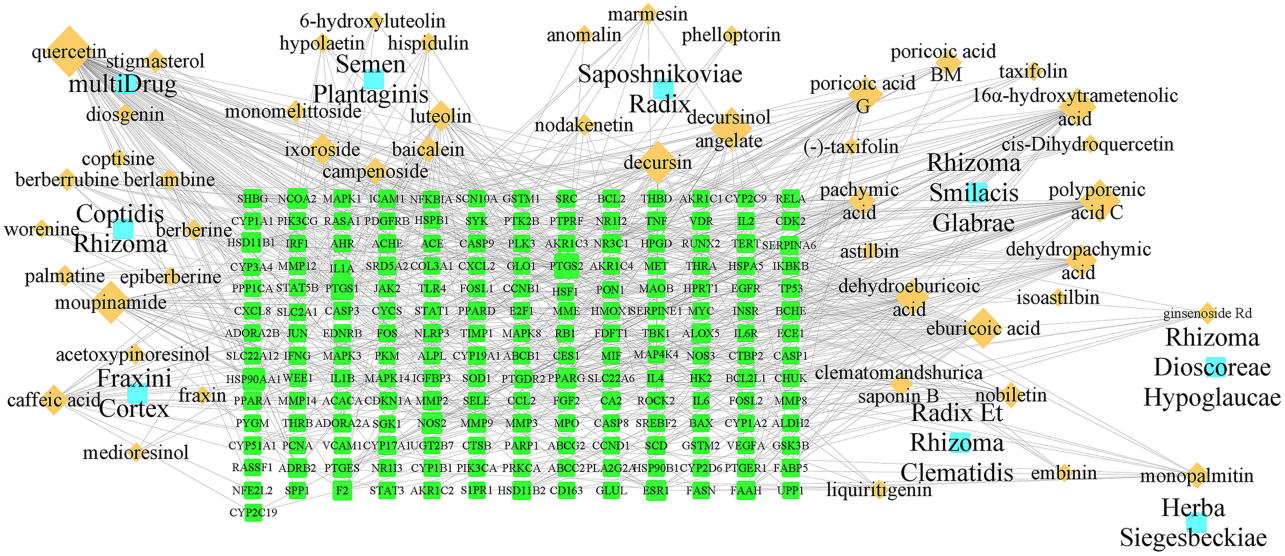

Figure 4 Chinese medicine - Compounds - Potential target network.

Construction of PPI Network and Determination of Key Targets

Import the protein interaction data of intersection targets into Cytoscape 3.8.0 to build a PPI network (Figure 5a) (including 182 nodes, 3273 edges). Calculate DCs of 182 target proteins using the plug-in CytoNCA, and subnetworks of 74 target proteins were screened according to DC ≥35.76 (mean) (Figure 5b). Then calculate DC, BC, CC, EC and LAC of 74 target proteins in the sub-network again as above. According to DC ≥48.46 (mean), BC ≥24.54 (mean), CC ≥0.76 (mean), EC ≥0.11 (mean), LAC ≥37.14 (mean), 25 target proteins were screened out (Figure 5c). The key target proteins included IL-1β, NFKBIA, IL-6, TNF, CXCL8, MMP9, etc.

GO Functional and KEGG Pathway Enrichment Analyses

The 2733 entries, including 2509 BP, 38 CC and 186 MF were from GO functional enrichment analysis of 183 intersection targets. The main focus of BP lies in the reaction to lipopolysaccharide and the response to bacterial-derived molecules; CC primarily occurred in membrane raft and membrane microdomain; MF was associated with heme binding and oxidoreductase activity. Based on $P < 0.05$, Figure 6 illustrates the visual representation of the top 10 distinct biological process items that were chosen. One hundred and seventy-two pathways were from KEGG functional enrichment analysis, and according to the *P* value,

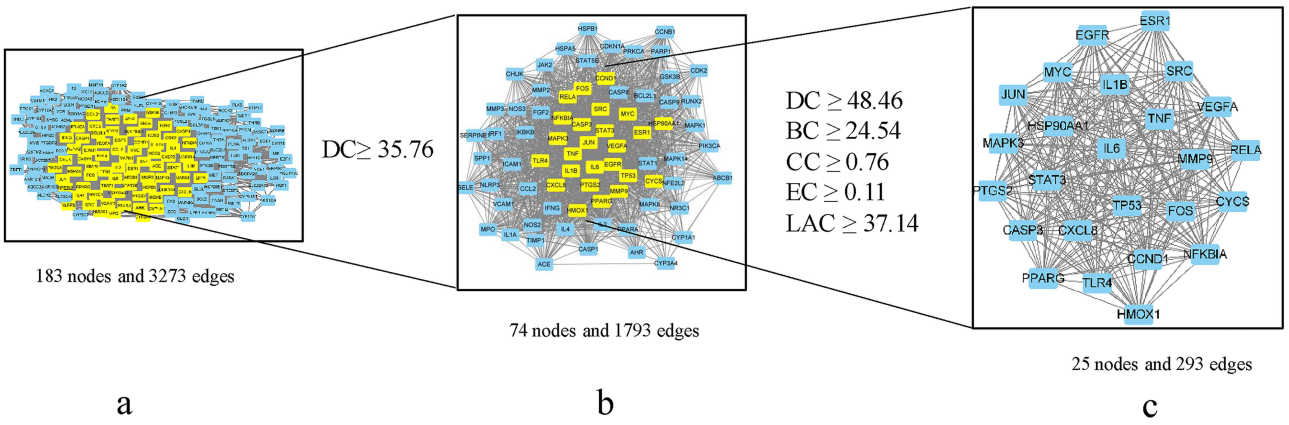

Figure 5 The PPI network filtering process; Note: (**a**) The intersection targets of Qinpi Tongfeng formula and AGA; (**b**) Targets after DC screening; (**c**) : Potential core targets of Qinpi Tongfeng formula in regulating AGA.

Figure 6 GO functional enrichment analysis; Notes: The horizontal coordinate represents the number of selected targets contained in each item and the corresponding percentage of the total number of targets. The vertical coordinate is the name of the biological processes (BP), cellular components (CC) and molecular functions (MF). The top 10 significant GO analyses are listed. Q value is the p value after multiple hypothesis test correction. When the q value smaller, the more significant enrichment of GO function.

the visual representation included a selection of the top 30 (Figure 7). In Figures 6 and 7, colors represented enrichment significance, with darker colors representing more significant enrichment of targets in this pathway and smaller *P*-values. The top 4 pathways were Lipid and atherosclerosis, Hepatitis B, AGE-RAGE signaling pathway in diabetic complications, and Kaposi sarcoma-associated herpesvirus infection, which had little correlation with AGA, while IL-17 was the most enriched inflammatory pathway.

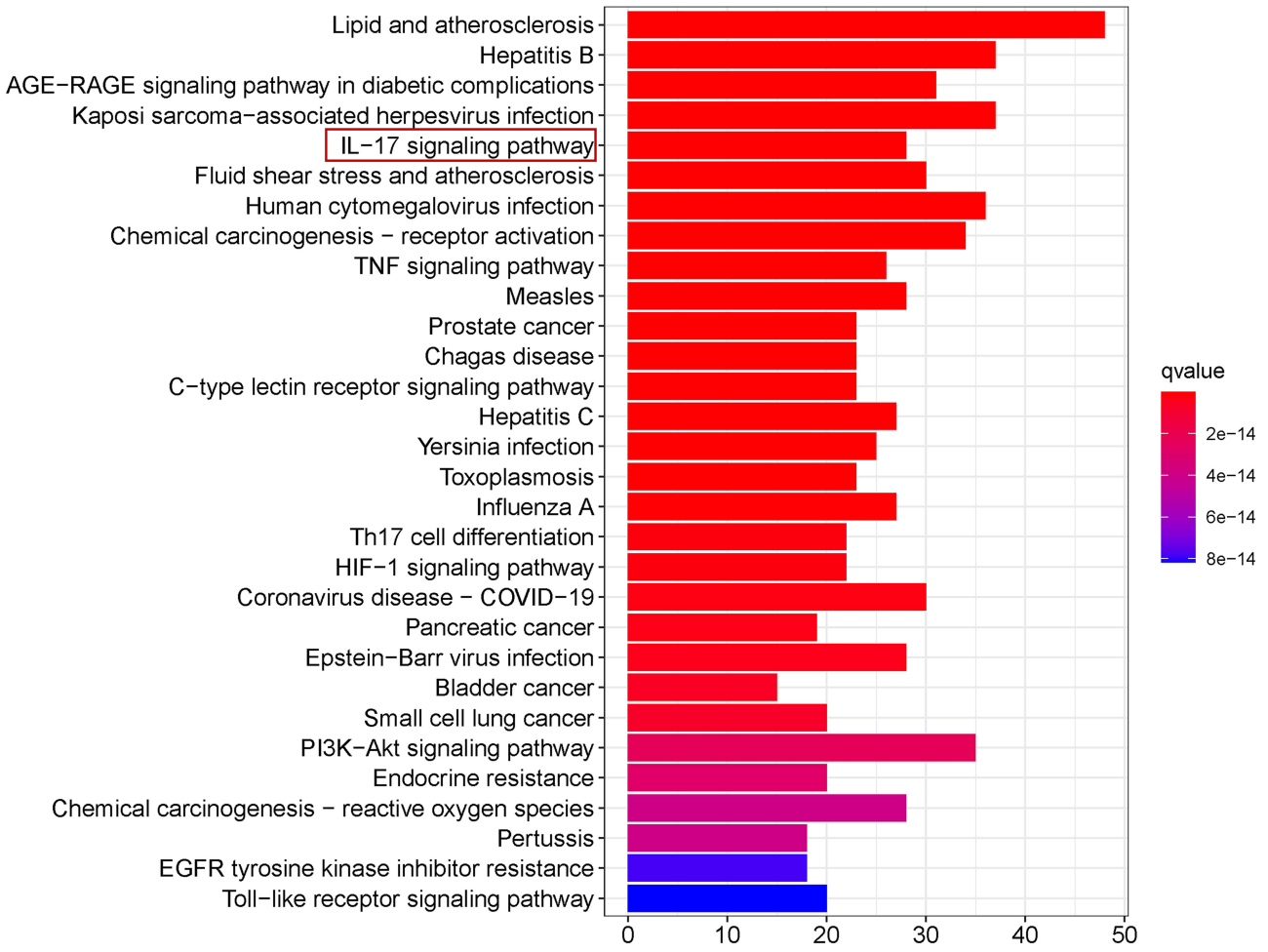

Figure 7 KEGG pathway enrichment analysis. Notes: The horizontal coordinate represents the number of selected targets contained in each item and the corresponding percentage of the total number of targets. The vertical coordinate is the name of the signaling pathway and disease. The top 30 significant KEGG analyses are listed. Q value is the p value after multiple hypothesis test correction. When the q value smaller, the more significant enrichment of signaling pathway.

Molecular Docking of the Potential Active Compounds of the Qinpi Tongfeng Formula and Core Proteins

Through molecular docking, this study found that the binding energy of quercetin, eburicoic acid and polyporenic acid C with 25 core targets were all less than 0. In addition, the binding energy of 73 pairs of components and core target molecular docking was ≤-5.0kJ/mol, and that of 59 pairs of components and core target molecular docking was ≤-7.0kJ/mol. See Table 3 for specific results.

Experimental Results

General Observation of Rats

Before modeling, the rats in each group were in good mental state and diet state, and their fur was shiny. After modeling, the right paw of the N group was slightly curled but there was no redness or swelling. The rats in the other 5 groups showed varying degrees of decreased activity, poor mental state, reduced water and food intake, weight loss, and inflammation and edema and claudication of their ankle joints. The right foot performance of the rats in the MSU group and the N group after modeling is shown in Figure 8.

Table 3 The Binding Energy of the Main Potential Active Compounds in the Qinpi Tongfeng Formula

Core Targets	Quercetin (kcal/mol)	Eburicoic Acid (kcal/mol)	Polyporenic Acid C (kcal/mol)
CASP3	−8.0	−7.3	−7.5
CCND1	−7.5	−8.0	−9.0
CXCL8	−6.2	−5.8	−5.6
CYCS	−7.2	−7.6	−7.7
EGFR	−7.9	−8.2	−8.2
ESR1	−8.4	−8.3	−7.5
FOS	−7.2	−7.2	−7.5
HMOX1	−4.9	−4.8	−5.1
HSP90AA1	−7.5	−6.2	−7.0
IL1B	−7.1	−6.1	−7.2
IL6	−6.9	−7.2	−7.1
JUN	−5.5	−6.4	−5.4
MAPK3	−8.3	−7.7	−8.6
MMP9	−8.4	−7.8	−7.6
MYC	−6.5	−7.0	−7.0
NFKBIA	−7.7	−8.0	−7.6
PPARG	−8.1	−7.9	−8.4
PTGS2	−9.7	−9.2	−9.3
RELA	−7.5	−7.1	−8.0
SRC	−8.8	−8.8	−9.2
STAT3	−7.4	−7.3	−7.5
TLR4	−6.9	−6.2	−6.2
TNF	−10.4	−9.1	−9.8
TP53	−7.2	−7.2	−7.3
VEGFA	−7.0	−6.2	−7.2

Effect of Qinpi Tongfeng Formula on the Swelling Volume of Foot and Ankle in AGA Rats

The swelling volume of their right ankles in MSU group increased considerably at each time point ($P < 0.01$) vs N group, reached the peak at 12 h, and could be maintained until 96 h after modeling, indicating successful establishment and good stability of models. The swelling volume of their right ankles in QPTFF-M group, QPTFF-H group and MSU group considerably differred at different time points after 6 h ($P < 0.05$, $P < 0.01$) vs MSU group. The swelling volume of their right ankles in MSU group considerably differred at 48 h after ($P < 0.05$) vs QPTFF-L group. The smaller swelling volume of their right ankles was considerably seen in the QPTFF-M and QPTFF-H groups vs QPTFF-L group ($P < 0.01$) (Supplementary material Table S2 and Figure 9).

Effect of Qinpi Tongfeng Formula on Ankle Histopathology in AGA Rats

H&E staining results (Figure 10) showed no inflammatory cells infiltration such as monocytes and neutrophils of their ankle joint tissues of N group, and cells in the synovial layer were evenly arranged. Compared with the N group, synovial hyperplasia, capillary congestion and edema were obvious in the MSU group, and the infiltration of inflammatory cells such as monocytes and neutrophils was obvious. The above pathological conditions in the QPTFF-L, QPTFF-M, QPTFF-H and DFS groups were significantly improved vs MSU group, that is, inflammatory cell infiltration, synovial layer cell proliferation, capillary congestion and edema were significantly reduced.

Effect of Qinpi Tongfeng Formula on Serum Inflammatory Factors and MMP-9 in AGA Rats

The increased IL-17A, IL-1β, IL-6, IL-8, TNF-α and MMP-9 expression levels in the serum of MSU group were considerably seen ($P < 0.01$) vs N group. The decreased inflammatory factors and MMP-9 expression levels were considerably seen in QPTFF-L, QPTFF-M, QPTFF-H and DFS groups ($P < 0.05$, $P < 0.01$) vs MSU group. The lower

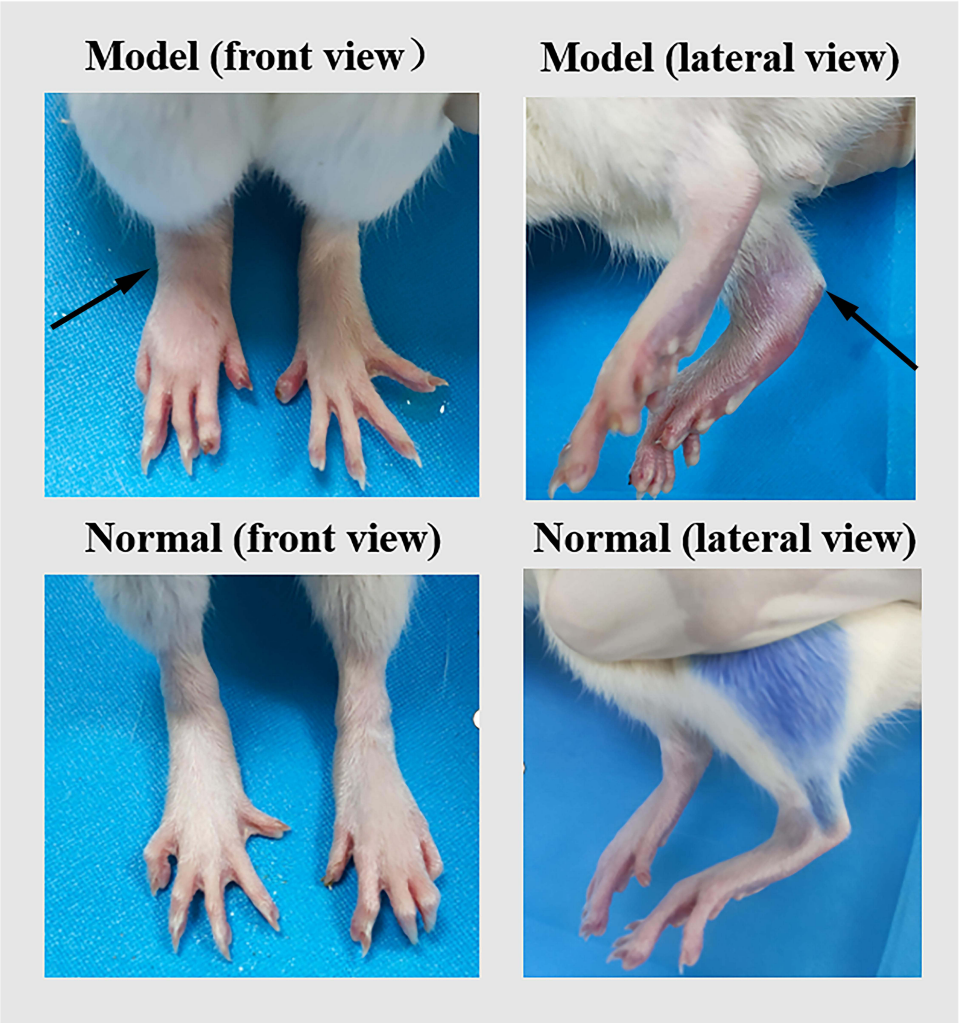

Figure 8 Right foot performance of rats in the MSU group and N group.

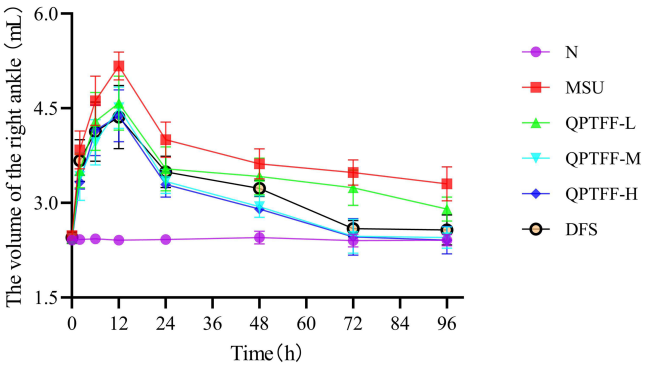

Figure 9 The volume changes of the right ankle in rats with AGA.

IL-6, IL-8, TNF-α and MMP-9 expression levels were considerably seen in the QPTFF-M group ($P < 0.05$, $P < 0.01$) vs QPTFF-L group. However, no notable variations observed in the serum inflammatory factors and MMP-9 levels were seen among the QPTFF-M, QPTFF-H and DFS groups ($P > 0.05$) (Figure 11).

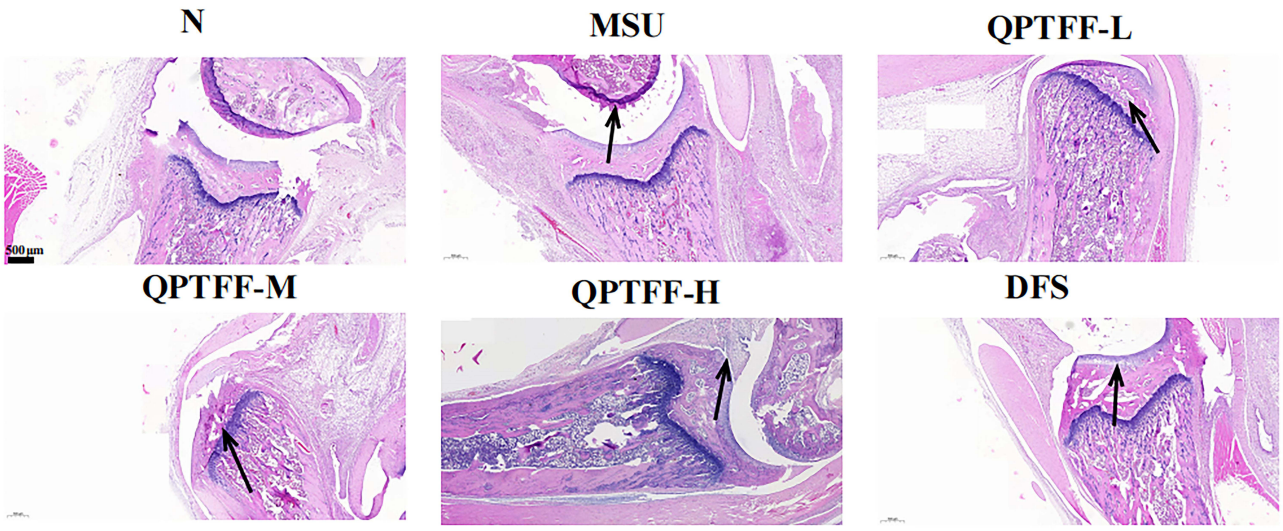

Figure 10 Pathological changes in rats with AGA (H&E staining, 25×, Scale 500 μm).

Effect of Qinpi Tongfeng Formula on mRNA of Related Targets in Ankle Joints

Measure IL-17A, IKK-β, NF-κB p65 and IL-6 mRNA expression levels in rats' ankle joints by qRT-PCR. The considerably increased IL-17A, IKK-β, NF-κB p65 and IL-6 mRNA expression levels of MSU group were seen ($P < 0.01$) vs N group. The considerably decreased IL-17A, IKK-β, NF-κB p65 and IL-6 mRNA expression levels in QPTFF-M, QPTFF-H and DFS groups were seen ($P < 0.05$, $P < 0.01$) vs MSU group. The lower IL-17A and IL-6 mRNA expression levels were considerably seen in the QPTFF-M group ($P < 0.05$) vs QPTFF-L group. However, no notable variations observed in the IL-17A, IKK-β, NF-κB p65 and IL-6 mRNA expression levels among the QPTFF-M, QPTFF-H and DFS groups ($P > 0.05$) (Figure 12).

Expression of Related Proteins Detected by Western Blot

Western blot analysis revealed expression level of IL-17A, IL-17RA, IKK-β, NF-κB p65, IL-6 protein and phosphorylation level of IKK-β and NF-κB p65 of rats with AGA. The considerably increased protein expression levels of IL-17A, IL-17RA and IL-6 and the levels of pNF-κB p65/NF-κB p65 and pIKK-β/IKK-β of MSU group were seen ($P < 0.01$) vs N group. The considerably decreased IL-17A, IL-17RA, IL-6 protein expression levels and the ratios of pNF-κB p65/NF-κB p65 and pIKK-β/ IKK-β were seen in QPTFF-M, QPTFF-H and DFS groups ($P < 0.01$) vs MSU group; The considerably decreased IL-17A protein expression and ratio of pNF-κB p65/NF-κB p65 in QPTFF-L group were seen ($P < 0.05$, $P < 0.01$). The considerably lower IL-17A, IL-17RA, and IL-6 protein expression levels of QPTFF-M group were seen ($P < 0.05$) vs QPTFF-L group, however, no notable variations observed in the IL-17A, IL-17RA, IL-6 protein expression levels and the levels of pNF-κB p65/NF-κB p65 and pIKK-β/IKK-β among the QPTFF-M, QPTFF-H and DFS groups ($P > 0.05$) (Figure 13).

Pathological Results of Rat Liver and Kidney Tissues

The liver capsule remained undamaged and the hepatic lobular architecture was present in the N group, the hepatic cords were arranged smoothly, there was no necrosis of hepatocytes, a small amount of hepatocyte cytoplasm was loose and lightly stained and balloon-like lesions, and no obvious inflammatory cell infiltration in hepatocytes and hepatic sinusoids be seen. The structure of portal area was relatively complete without fibrous tissue proliferation. No pathological changes were also observed in the QPTFF-H group, similar to the findings in the N group (Figure 14A).

In the N group, the renal capsule was intact, the boundary between cortex and medulla was clear, and scattered glomeruli were seen. The glomerular structure was complete and clear, and no glomerular basal thickening and inflammatory exudation were observed. Some renal tubular epithelial cells showed degeneration. There was no fibrous tissue proliferation in the stroma. No pathological changes were also observed in the QPTFF-H group, and similar to the findings in the N group (Figure 14B).

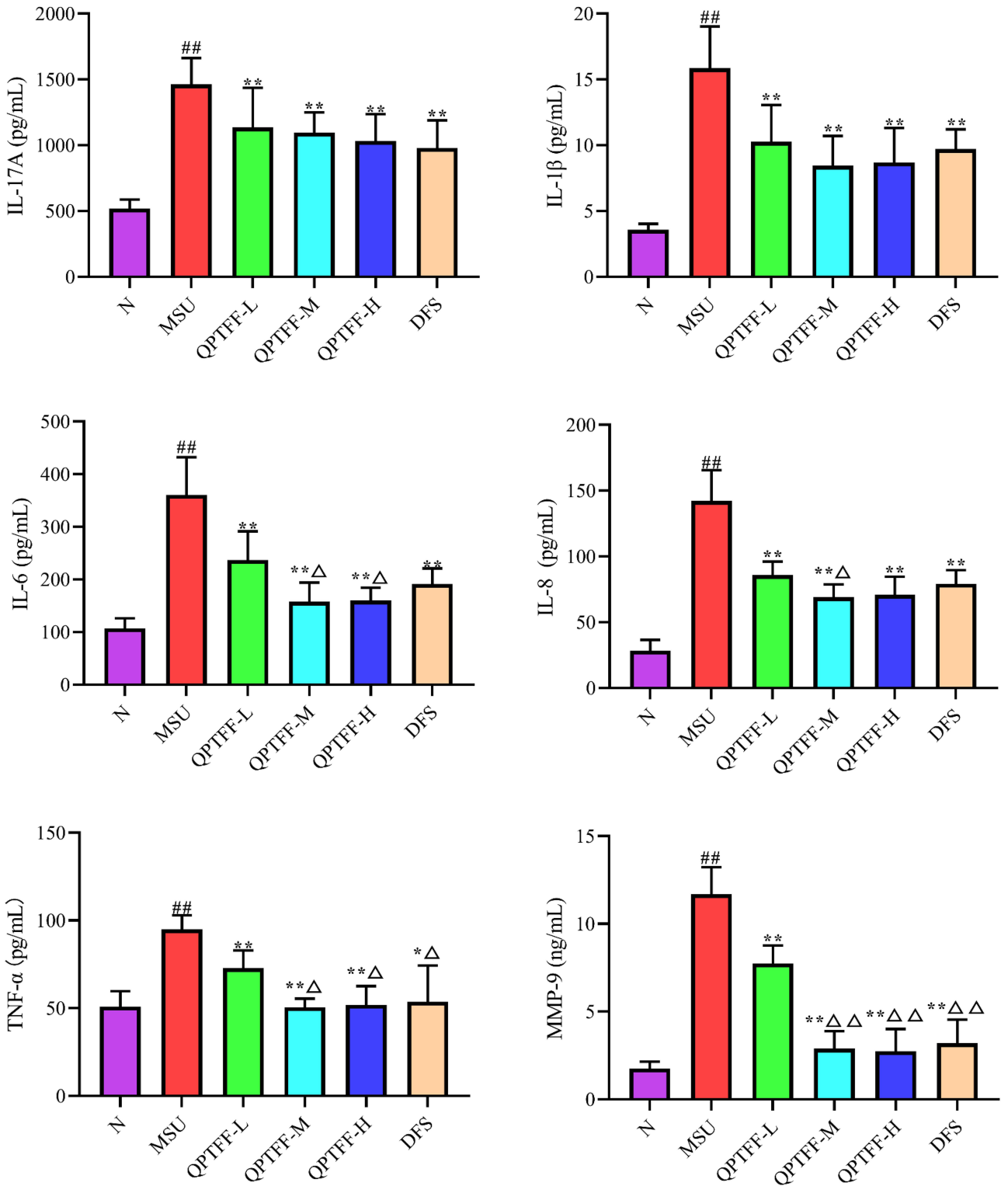

Figure 11 Inflammatory factors and MMP-9 expression in serum of rats with AGA (Mean ±SD, *n* = 6).
Notes: ##*P*<0.01 vs N group; **P*<0.05, ***P*<0.01 vs MSU group; Δ*P*<0.05, ΔΔ*P*<0.01 vs QPTFF-L group.

Discussion

Potential Mechanism of QPTFF in Treating AGA

Qinpi Tongfeng formula possesses the abilities to eliminate heat and purify toxins, and specialize in dehumidifying turbidity, alleviating arthralgia and stopping pain, and has a good curative effect on AGA.[36] Fifty-five compounds were

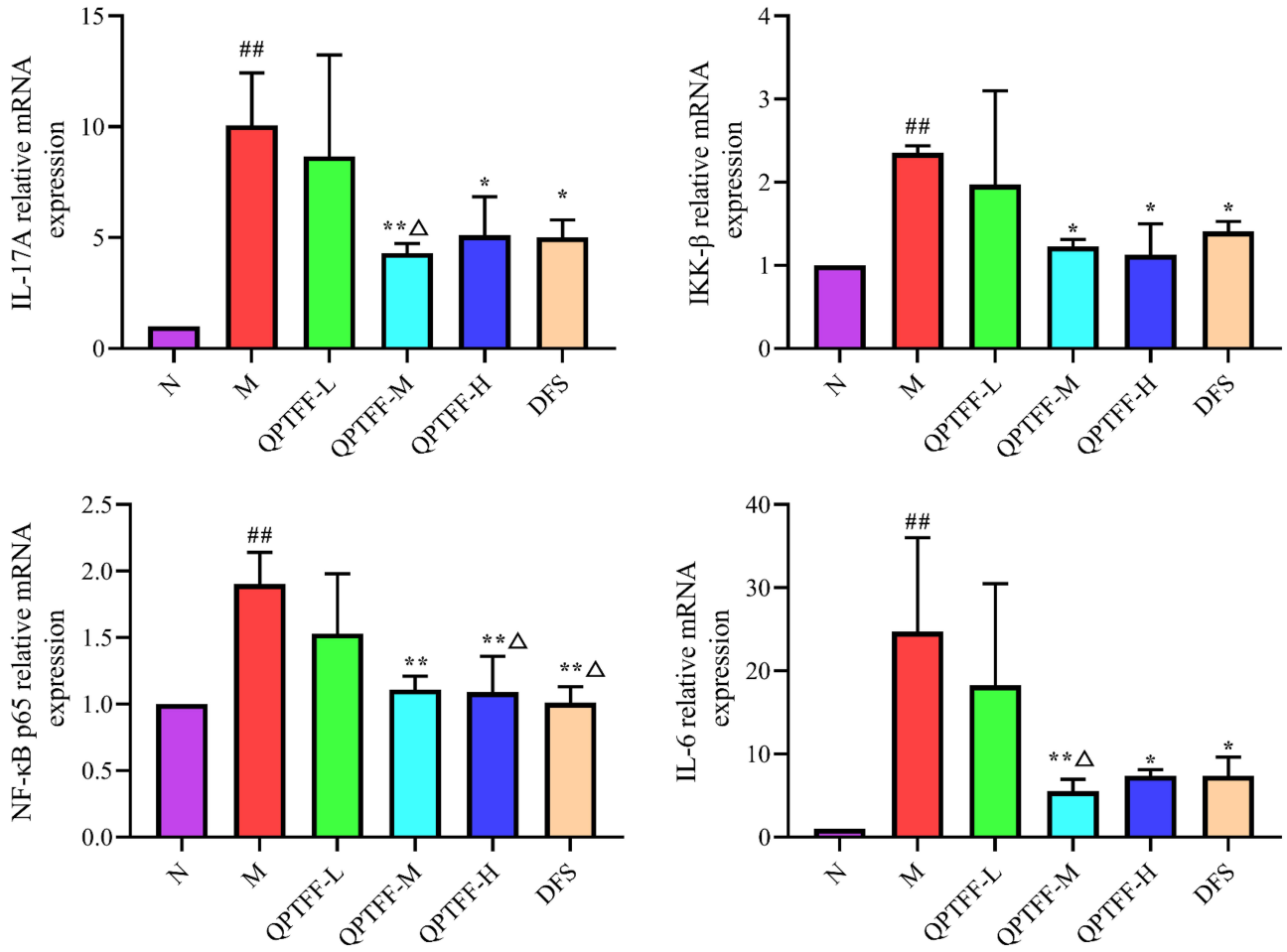

Figure 12 mRNA relative expression levels of IL-17A, IL-6, IKK-β and NF-κB p65 in ankle tissues of rats with AGA (Mean ±SD, n = 3).
Notes: ##*P*<0.01 vs N group; **P*<0.05, ***P*<0.01 vs MSU group; △*P*<0.05 vs QPTFF-L group.

obtained from QPTFF, with 183 potential targets in treating AGA. The network map of "Chinese medicine-Compounds-Potential target" was constructed by network pharmacology, and it was found that different drugs had common compounds, and different compounds also had common targets. Tufuling (*Rhizoma Smilacis Glabrae*), Cheqianzi (*Semen Plantaginis*) and Xixiancao (*Herba Siegesbeckiae*) had common compounds, such as quercetin, and most of the regulated targets, indicating the synergistic effect between Chinese medicines. In addition, Tufuling (*Rhizoma Smilacis Glabrae*) and Bixie (*Rhizome Dioscoreae Hypoglaucae*) also had a common compound, diosgenin, which regulated 14 targets, showing its important role in treating AGA. Based on the degree measurement, the top 3 were quercetin, eburicoic acid and polyporenic acid C, being the possible primary QPTFF-related compounds in treating AGA. Among them, quercetin acted on 77 potential targets, which came from Cheqianzi (*Semen Plantaginis*), Tufuling (*Rhizoma Smilacis Glabrae*) and Xixiancao (*Herba Siegesbeckiae*); Eburicoic acid was found to act on 37 potential targets from Tufuling (*Rhizoma Smilacis Glabrae*); Polyporenic acid C was found to act on 35 potential targets and was derived from Tufuling (*Rhizoma Smilacis Glabrae*). All of these compounds were found in Tufuling (*Rhizoma Smilacis Glabrae*), so the important role of Tufuling (*Rhizoma Smilacis Glabrae*) can be seen. Studies have found that quercetin can improve the acute inflammatory manifestations of urate crystal-induced AGA model rats, inhibit the recruitment of white blood cells, reduce the levels of chemokines and malondialdehyde, the end product of lipid peroxidation, and increase the activities of antioxidant enzymes.[37] Although our study selected quercetin as a potential target for QPTFF, due to its low solubility in water, its bioavailability is influenced by the type of glycosides present in different food sources.[38] Studies have indicated that quercetin is soluble in alcohol and lipids, suggesting that quercetin may need to be

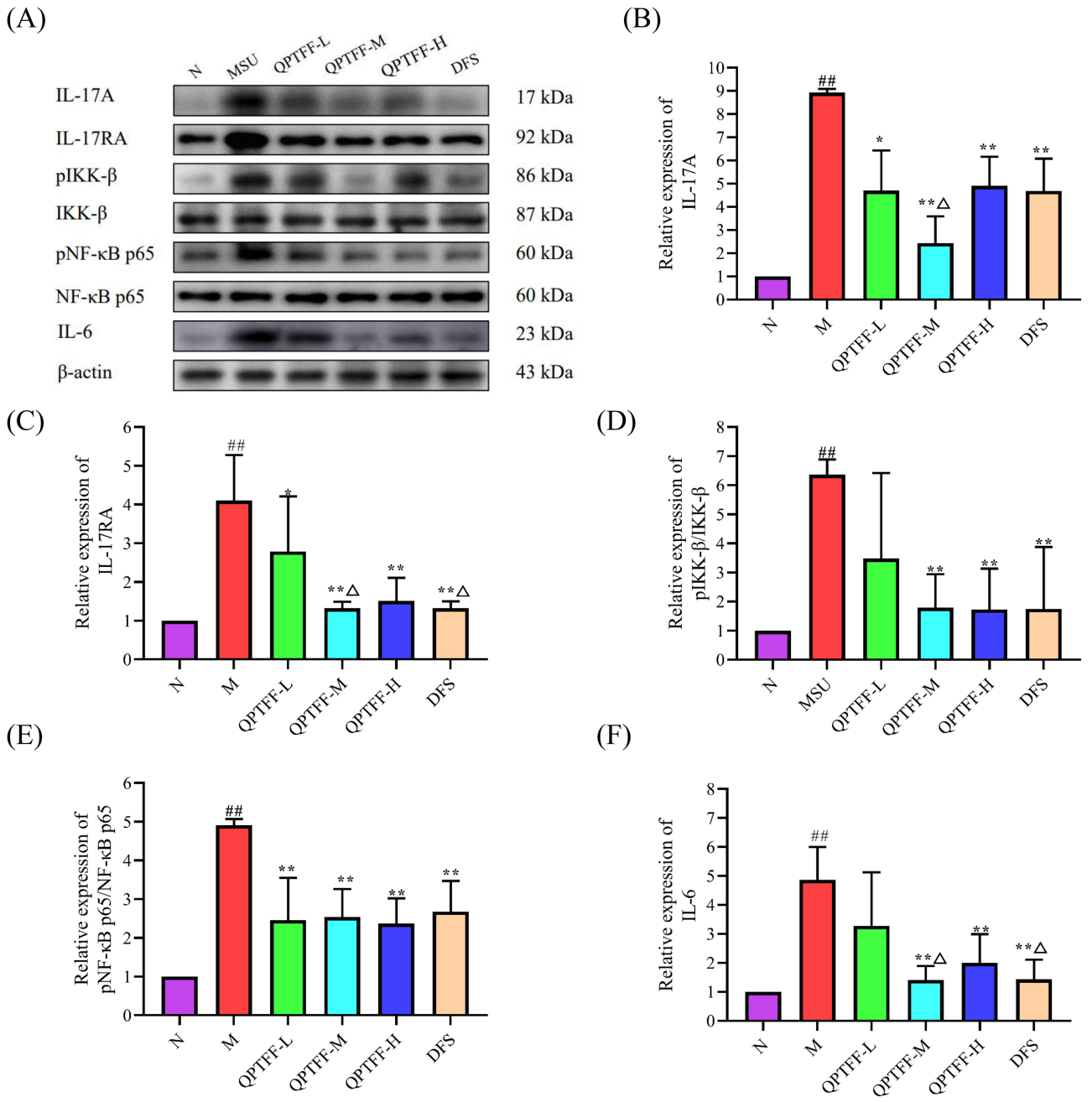

Figure 13 Relative expression levels of related proteins in tissues of rats ankle joints with AGA (Mean±SD, n = 3).
Notes: (**A**): Western blot strip of IL-17A, IL-17RA, pIKK-β, IKK-β, pNF-κB p65, NF-κB p65 and IL-6 protein; (**B–F**) histogram of statistical results of IL-17A, IL-17RA, pIKK-β/IKK-β, pNF-κB p65/NF-κB p65 and IL-6 proteins, respectively; $^{\#\#}P<0.01$ vs N group; $^{*}P<0.05$, $^{**}P<0.01$ vs MSU group, $^{\Delta}P<0.05$ vs QPTFF-L group.

administered through modified dosage forms, such as the use of nanocarrier systems, to improve its effectiveness and bioavailability in the treatment of arthritis and gouty arthritis.[39] Research findings indicate that eburicoic acid exhibits properties of an antioxidant and possesses anti-inflammatory effects.[40] Eburicoic acid has an obvious anti-inflammatory effect by inhibiting the activation of PI3K/Akt/NF-κB signaling pathway,[41] furthermore, it possesses the ability to suppress xanthine oxidase activity, leading to low uric acid levels.[42] Polyporenic acid C inhibits the inducible NO synthase expression and reduces the level of NO to achieve anti-inflammatory effect.[43,44]

After two topological screenings through the PPI network, 25 core target proteins were finally obtained, among which IL-1β, NFKBIA, IL-6, TNF, CXCL8 and MMP9 being the possible key QPTFF-target proteins in treating AGA. The molecular

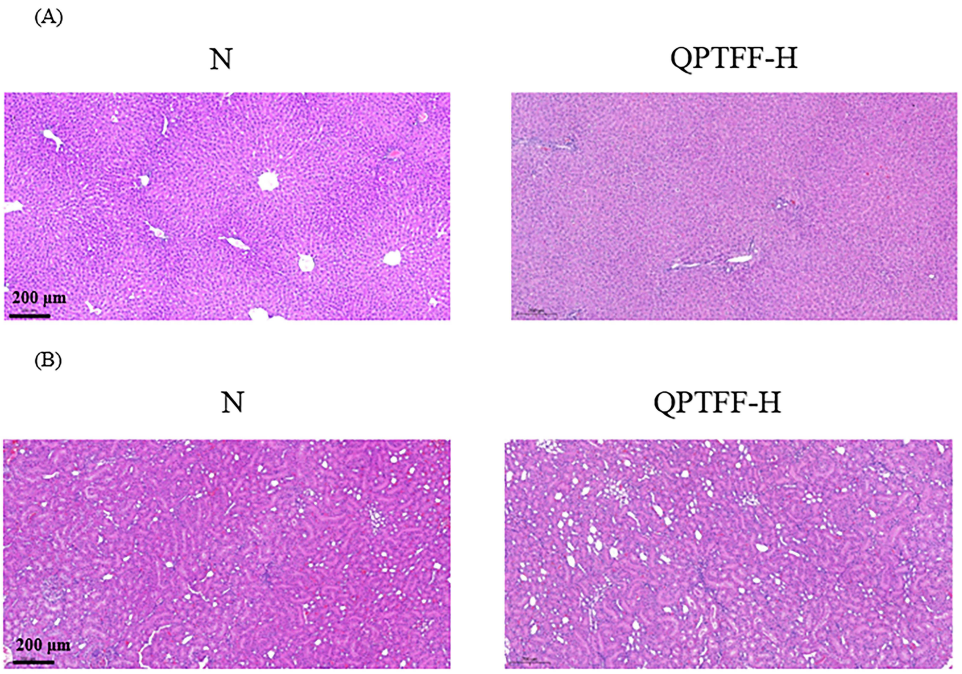

Figure 14 Pathological changes of liver and kidney tissues of rats (H&E staining, 200×, Scale 50 μm). (**A**): liver tissue; (**B**): kidney tissue.

docking analysis revealed that quercetin, eburicoic acid, and polyporenic acid C exhibited robust binding affinity towards the 25 core target proteins. IL-1β is an important inflammatory factor mediating GA.[45] As a key cytokine, IL-1β initiates inflammation and is significantly helpful in progression of AGA. The expression of IL-1β can be suppressed to mitigate the inflammatory response in AGA.[46] *NFKB1A*-encoded NF-κB IκBα is an inhibitor that regulates the movement of transcription factor NF-κB into and out of the nucleus, and NF-κB specializes in the regulation of crucial cytokine expression in AGA.[47] IL-1β released in AGA patients can induce an inflammatory reaction and subsequently enhance the NF-κB activation, and the reciprocal nature of the activity is evident as NF-κB signaling induces an upregulation in pro-IL-1β.[48] Studies have found the considerably higher IL-1β, IL-6, IL-8 and TNF-α serum levels in GA patients,[49] and IL-6 is related to the onset of GA and tophus formation.[50] IL-6 exhibits a cooperative impact with IL-1β and TNF-α, resulting in the production of vascular endothelial growth factor. This factor influences vascular endothelial cells, causing an elevation in their permeability. Consequently, it contributes to the escalation of joint swelling.[51] TNF-α belongs to the family of tumor necrosis factors, and in human neutrophils stimulated with TNF-α, MSU stimulation leads to significant secretion of IL-1β.[52] CXCL8, named IL-8, promotes development of inflammation in the pathogenesis of GA.[53] MMP-9 can degrade the extracellular matrix, cause synovial inflammation of the joint, and destroy the joint.[54]

KEGG enrichment analysis results indicates IL-17 signaling pathway as the most enriched inflammatory pathway. Anti-inflammatory and cartilage protective effects of QPTFF could potentially contribute to the treatment of AGA. Studies have shown that inhibition of IL-17 expression can reduce joint erosion in animal models of arthritis.[55] In the early stages of gout symptoms in AGA patients, serum IL-17 levels were significantly increased.[56] NF-κB p65 signaling pathway is the subsequent pathway of IL-17 signaling pathway. Among the members of the IL-17 family, IL-17A stands out as both the inaugural and extensively researched member to date. It can promote T cells, epithelial cells and other cells to synthesize, secrete lots of cytokines (ig.IL-6, IL-8), thereby aggravating the inflammatory response and leading to tissue damage.[57–59] Studies have confirmed the existence of IL-17A in both the serum and synovial tissue among individuals diagnosed with different forms of arthritis, strong correlation between this cytokine and the development of the disease.[60,61] Hence, we opted to investigate the IL-17A/NF-κB p65 signaling pathway a means of elucidating the mode of action of QPTFF in treating AGA rats.

Effect of Qinpi Tongfeng Formula on IL-17A/NF-κB p65 Signaling Pathway

IL-17A activates the classical NF-κB pathway. In response to an external stimulus, IL-17A binds to its receptor to form a receptor complex, transmitting signals and recruiting NF-κB activator 1 (Act1) to the receptor complex, meanwhile, TNF receptor-associated factor 6 (TRAF6) is also recruited to the receptor complex and ubiquitinated; Ubiquitinated TRAF6 induces TAK1 phosphorylation and activation; The activated TAK1 can further phosphorylate IKKβ, thereby activating IKK complex and ultimately activating NF-κB; Activated NF-κB enters the nucleus, enhances the transcription level of target genes, regulates the expression level of downstream genes, and facilitates the release of pro-inflammatory cytokines such as IL-1β, TNF-α, IL-6, IL-8 and MMP9,[61,62] stimulation of IL-1β and TNF-α in turn enhances the phosphorylation of IKKβ. Thus, the vicious cycle aggravates inflammation;[63] Repeated inflammatory stimulation can cause joint swelling and pain and bone destruction of painful joints in GA patients, which greatly influences the emergence and progression of GA.[64] Therefore, the IL-1β, IL-6, IL-8, TNF-α and MMP9' serum contents can reflect the degree of inflammation in rats to a certain extent, and illustrate the significant help of intervention of IL-17A/ NF-κB p65 signaling pathway in treating AGA.

The anti-inflammatory effect of QPTFF was confirmed in the rat experiment conducted in this study, providing validation for the network pharmacology findings. In the rat experiment, in addition to the intervention of AGA rats with QPTFF, diclofenac sodium, a commonly used drug for clinical treatment of AGA, was added. The IL-17A, IL-1β, IL-6, IL-8, TNF-α and MMP-9 expression levels in serum were significantly reduced by medium and high doses of QPTFF and diclofenac sodium. Compared with the diclofenac sodium group, no notable disparities were observed in the serum levels of inflammatory factors and MMP-9 between the QPTFF-M and QPTFF-H groups, suggesting that QPTFF and diclofenac sodium have similar effects in suppressing the manifestation of IL-17A, IL-1β, IL-6, IL-8, TNF-α and MMP-9. The considerably increased IL-17A, IL-6, IKK-β and NF-κB p65 mRNA expression levels of the MSU group were seen. The IL-17A, IL-17RA, IKK-β, NF-κB p65 and IL-6 protein expression levels, as well as the pIKK-β and pNF-κB p65 levels were also significantly increased, suggesting that IL-17A/NF-κB p65 signaling pathway was closely related to AGA. The considerably decreased IL-17A, IL-6, IKK-β and NF-κB p65 mRNA expression levels of the QPTFF-M and QPTFF-H groups were seen vs the MSU group. The considerably decreased IL-17A, IL-17RA, IKK-β, NF-κB p65, IL-6 protein expression levels and IKK-β and NF-κB p65 phosphorylation levels were also seen. These findings indicated that the involvement of QPTFF in the-17A/NF-κB65 signaling pathway could potentially contribute to the treatment of AGA. There are still some shortcomings in our study. We did not carry out experimental verification on all 25 core targets. Only relevant targets on the IL-17A/NF-κB p65 signaling pathway were selected for verification. In addition, in our experiment, we did not use the blocker of the pathway for experimental verification. In future research, we will further explore the mechanism of action of Qinpi Tongfeng Formula.

Conclusion

The main targets of QPTFF are IL-1β, NFKBIA, IL-6, TNF-α, CXCL8, MMP9, etc. QPTFF can greatly alleviate the joint inflammation of AGA rats, and high dose of QPTFF has no liver or kidney toxicity. The IL-17A/NF-κB p65 signaling pathway is implicated in the anti-inflammatory effects of QPTFF for treating AGA.

Data Sharing Statement

All drug compounds and related disease targets data were available from public databases and can also be available from the corresponding author upon receiving a reasonable request. (Wei Liu: fengshiliuwei@163.com).

Ethical Approval

All experiments were conducted in accordance with the ARRIVE (Animal in Research: In Vivo Experiments) guidelines and followed the principles set by the International Association for the Study of Pain (IASP) Research and Ethics. The animal experiment was approved by the Animal Ethics Committee of Tianjin University of TCM (TCM-LAEC2021137). And this study was approved by the Ethics Committee of First Teaching Hospital of Tianjin University of Traditional Chinese Medicine (TYLL2021[Z]017).

Acknowledgment

Yihua Fan, Wei Liu, and Yue Jin are co-first author. The authors express their gratitude to Ping Xin (Tianjin University of TCM) for her valuable assistance in refining the English language used in this paper. The authors express their gratitude to Yue Ji (First Teaching Hospital of Tianjin University of Traditional Chinese Medicine) for her contribution.

Author Contributions

All authors made a significant contribution to the work reported, whether that is in the conception, study design, execution, acquisition of data, analysis and interpretation, or in all these areas; took part in drafting, revising or critically reviewing the article; gave final approval of the version to be published; have agreed on the journal to which the article has been submitted; and agree to be accountable for all aspects of the work.

Funding

This received financial support from the National Natural Science Foundation of China (No. 82074377 and No. 82305202), the Qihuang Project under the Traditional Chinese Medicine Inheritance and Innovation "Hundred Million" Talent Program (Chinese Medicine People's Education Letter [2018] No. 12) - Liu Wei Qihuang Studio Construction Project, and Inheritance studio project of national famous old Chinese medicine experts(No.975022), the National Administration of Traditional Chinese Medicine Collaborative Project for Treating Major and Difficult-to-Treat Diseases with Integration of Traditional Chinese Medicine and Western Medicine (Gout and Hyperuricemia)..

Disclosure

The authors report no conflicts of interest in this work.

References

1. Johannsdottir GA, Palsson O, Jonsson H, et al. Guðrún Arna Jóhannsdóttir læknir, Ólafur Pálsson læknir, Helgi Jónsson læknir, Björn Guðbjörnsson læknir.Þvagsýrugigt-læknanleg liðbólga [Gout - a treatable condition]. *Laeknabladid*. 2018;104(4):177–186. Estonian. doi:10.17992/lbl.2018.04.181
2. Kaly L, Bilder I, Rozenbaum M, et al. Acute Gout Sacroiliitis. *Isr Med Assoc J*. 2021;23(3):191–192.
3. Mei Y, Dong B, Geng Z, Xu L. Excess Uric Acid Induces Gouty Nephropathy Through Crystal Formation: a Review of Recent Insights. *Front Endocrinol*. 2022;13:911968. doi:10.3389/fendo.2022.911968
4. Ejaz AA, Nakagawa T, Kanbay M, et al. Hyperuricemia in kidney disease: a major risk factor for cardiovascular events, vascular calcification, and renal damage. *Semin Nephrol*. 2020;40(6):574–585. doi:10.1016/j.semnephrol.2020.12.004
5. Xia Y, Wu Q, Wang H, et al. Global, regional and national burden of gout, 1990–2017: a systematic analysis of the Global Burden of Disease Study[J]. *Rheumatology*. 2020;59(7):1529–1538. doi:10.1093/rheumatology/kez476
6. FitzGerald JD, Dalbeth N, Mikuls T, et al. 2020 American college of rheumatology guideline for the management of gout. *Arthritis Care Res*. 2020;72(6):744–760. doi:10.1002/acr.24180
7. Kim HW, Joo YS, Yun HR, et al. Colchicine use and the risk of CKD progression: a multicentre nested case-control study. *Rheumatology*. 2022;61(11):4314–4323. doi:10.1093/rheumatology/keac077
8. Wu J, Liu Z. Progress in the management of acute colchicine poisoning in adults. *Intern Emerg Med*. 2022;17(7):2069–2081. doi:10.1007/s11739-022-03079-6
9. Gelber AC. Treatment Guidelines in Gout. *Rheum Dis Clin North Am*. 2022;48(3):659–678. doi:10.1016/j.rdc.2022.04.003
10. Wang HY, Yu TY. The similarities and differences of gout cognition in ancient books of qin and han dynasties. *Acta Chin Med Pharm*. 2017;45(5):114–118.
11. Liu W, Zeng P, Wu Y, et al. Diagnosis and treatment of gouty arthritis with traditional Chinese and Western medicine. *Rheumatism Arthritis*. 2021;10(5):62–65+72.
12. Liu L, Wang D, Liu M, et al. The development from hyperuricemia to gout: key mechanisms and natural products for treatment. *Acupunct Herbal Med*. 2022;2(1):25–32. doi:10.1097/HM9.0000000000000016
13. Ren S, Meng F, Liu Y, et al. Effects of external application of compound Qingbi granules on acute gouty arthritis with dampness-heat syndrome: a randomized controlled trial. *Chin Med*. 2020;15(1):117. doi:10.1186/s13020-020-00398-8
14. Wang Y, Xu Y, Tan J, et al. Anti-inflammation is an important way that Qingre-Huazhuo-Jiangsuan recipe treats acute gouty arthritis. *Front Pharmacol*. 2023;14:1268641. doi:10.3389/fphar.2023.1268641
15. Cao L, Zhao T, Xue Y, et al. The anti-inflammatory and uric acid lowering effects of Si-Miao-San on gout. *Front Immunol*. 2022;12:777522. doi:10.3389/fimmu.2021.777522
16. Fan Y, Liu W, Lu H, et al. Efficacy and safety of qinpi tongfeng formula in the treatment of acute gouty arthritis: a double-blind, double-dummy, multicenter, randomized controlled trial. *Evid Based Complement Alternat Med*. 2022;2022:7873426. doi:10.1155/2022/7873426
17. Zhang B, Dan W, Zhang G, et al. Molecular mechanism of gleditsiae spina for the treatment of high-grade serous ovarian cancer based on network pharmacology and pharmacological experiments. *Biomed Res Int*. 2022;2022:5988310. doi:10.1155/2022/5988310

18. Fan Y, Liu W, Jin Y, et al. Integrated molecular docking with network pharmacology to reveal the molecular mechanism of simiao powder in the treatment of acute gouty arthritis. *Evid Based Complement Alternat Med*. 2021;2021:5570968. doi:10.1155/2021/5570968
19. Daina A, Michielin O, Zoete V. SwissADME: a free web tool to evaluate pharmacokinetics, drug-likeness and medicinal chemistry friendliness of small molecules. *Sci Rep*. 2017;7(1):42717. doi:10.1038/srep42717
20. Egbuna C, Patrick-Iwuanyanwu KC, Onyeike EN, et al. FMS-like tyrosine kinase-3 (FLT3) inhibitors with better binding affinity and ADMET properties than sorafenib and gilteritinib against acute myeloid leukemia: in silico studies. *J Biomol Struct Dyn*. 2021;40(22):1–12.
21. Feng S, Zhang XD, Qin YY, et al. Study on the anti-tumor mechanism of daphnetin based on network pharmacology analysis and experimental verification in vitro. *Natural Product Res Develop*. 2022;34(1):144–152.
22. Yang Y, Dong Y, Chawla NV. Predicting node degree centrality with the node prominence profile. *Sci Rep*. 2014;4(1):7236. doi:10.1038/srep07236
23. Raman K, Damaraju N, Joshi GK. The organisational structure of protein networks: revisiting the centrality-lethality hypothesis. *Syst Synth Biol*. 2014;8(1):73–81. doi:10.1007/s11693-013-9123-5
24. Zhou T, Zhou Y, Ge D, et al. Decoding the mechanism of Eleutheroside E in treating osteoporosis via network pharmacological analysis and molecular docking of osteoclast-related genes and gut microbiota. *Front Endocrinol*. 2023;14:1257298. doi:10.3389/fendo.2023.1257298
25. Coderre TJ, Wall PD. Ankle joint urate arthritis (AJUA) in rats: an alternative animal model of arthritis to that produced by Freund's adjuvant. *Pain*. 1987;28(3):379–393. doi:10.1016/0304-3959(87)90072-8
26. Liu YF, Chen Z, Tu SH. Effect of flavored Simiao formula on the expression of NLRP3 mRNA and IL-1 β and TNF- α in the ankle tissues of rat model of hyperuricemia combined with acute gouty arthritis. *J Tradit Chin Med*. 2020;61(14):1268–1272.
27. Yang Q, Wang Q, Deng W, et al. Anti-hyperuricemic and anti-gouty arthritis activities of polysaccharide purified from Lonicera japonica in model rats[J]. *Int J Biol Macromol*. 2019;123:801–809. doi:10.1016/j.ijbiomac.2018.11.077
28. Xu SY, Bian RL, Chen X. *Pharmacological Experimental Methodology*. 3rd ed. Beijing: The People's Health Publishing House; 2002:1860–1861.
29. Nie AZ, Lin ZJ, Zhang B. Progress on the chemical composition and pharmacological effects of Qinpi. *Chin Tradit Herbal Drugs*. 2016;47 (18):3332–3341.
30. He X, Yi T, Tang Y, et al. Assessing the quality of smilacis glabrae rhizoma (Tufuling) by colormetrics and UPLC-Q-TOF-MS. *Chin Med*. 2016;11 (33):1–9. doi:10.1186/s13020-016-0104-y
31. Tian PP, Zhang XX, Wang HP, et al. Rapid analysis of components in coptis Chinensis franch by ultra-performance liquid chromatography with quadrupole time-of-flight mass spectrometry. *Pharmacogn Mag*. 2017;13(49):175–179. doi:10.4103/0973-1296.197635
32. Guo L, Zeng SL, Zhang Y, et al. Comparative analysis of steroidal saponins in four Dioscoreae herbs by high performance liquid chromatography coupled with mass spectrometry. *J Pharm Biomed Anal*. 2016;117:91–98. doi:10.1016/j.jpba.2015.08.038
33. Ren WG, Wu LB, Jiang X, et al. Analysis on crude and wine-processed Siegesbeckia pubescens by UPLC-Q-TOF/MS. *Chin Tradit Herbal Drugs*. 2014;45(2):181–187.
34. Sun YJ, Huo ZP, Wang Y, et al. Based on UPLC-Q-TO F/MS~E to analyze the variation pattern of the chemical composition at different processing times. *Chin J Experi Tradit Med Formulae*. 2022;28(4):146–153.
35. Chen L, Chen X, Su L, et al. Rapid characterisation and identification of compounds in Saposhnikoviae Radix by high-performance liquid chromatography coupled with electrospray ionisation quadrupole time-of-flight mass spectrometry. *Nat Prod Res*. 2018;32(8):898–901. doi:10.1080/14786419.2017.1366482
36. Liu W, Wu YH, Zhang L, et al. Clinical randomized controlled trial of heat-clearing and detoxification, dampness and turbidity-removing method for gout. *China J Tradit Chin Med Pharm*. 2016;31(3):1113–1116.
37. Huang J, Zhu M, Tao Y, et al. Therapeutic properties of quercetin on monosodium urate crystal-induced inflammation in rat. *J Pharm Pharmacol*. 2012;64(8):1119–1127. doi:10.1111/j.2042-7158.2012.01504.x
38. Memariani H, Memariani M, Ghasemian A. Quercetin as a promising antiprotozoan phytochemical: current knowledge and future research avenues. *Biomed Res Int*. 2024;2024:7632408. doi:10.1155/2024/7632408
39. Tomou EM, Papakyriakopoulou P, Saitani EM, Valsami G, Pippa N, Skaltsa H. Recent advances in nanoformulations for quercetin delivery. *Pharmaceutics*. 2023;15(6):1656. doi:10.3390/pharmaceutics15061656
40. Huang GJ, Deng JS, Huang SS, et al. Hepatoprotective effects of eburicoic acid and dehydroeburicoic acid from Antrodia camphorata in a mouse model of acute hepatic injury. *Food Chem*. 2013;141(3):3020–3027. doi:10.1016/j.foodchem.2013.03.061
41. Wang YZ, Zhang L, Sun WJ, et al. Effect of eburicoic acid on adjuvant arthritis in rats. *Pharmacol Clini Chinese Mater Med*. 2016;32(2):23–27.
42. Zhang L, Wang YZ, Yu HL, et al. Effect of eburicoic acid on Xanthine oxidase activity in hyperuricemia. *Biotic Resources*. 2017;39(2):102–107.
43. Deng JS, Huang SS, Lin TH, et al. Analgesic and anti-inflammatory bioactivities of eburicoic acid and dehydroeburicoic acid isolated from Antrodia camphorata on the inflammatory mediator expression in mice. *J Agric Food Chem*. 2013;61(21):5064–5071. doi:10.1021/jf303820k
44. Lee SR, Lee S, Moon E, et al. Bioactivity-guided isolation of anti-inflammatory triterpenoids from the sclerotia of Poria cocos using LPS-stimulated Raw264.7 cells. *Bioorg Chem*. 2017;70:94–99. doi:10.1016/j.bioorg.2016.11.012
45. Fattori V, Staurengo-Ferrari L, Zaninelli TH, et al. IL-33 enhances macrophage release of IL-1β and promotes pain and inflammation in gouty arthritis. *Inflamm Res*. 2020;69(12):1271–1282. doi:10.1007/s00011-020-01399-x
46. Gong QY, Chen Y. Correlation between P2X7 receptor gene polymorphisms and gout. *Rheumatol Int*. 2015;35(8):1307–1310. doi:10.1007/s00296-015-3258-5
47. Hulin-Curtis SL, Sharif M, Bidwell JL, et al. Evaluation of NFKB1A variants in patients with knee osteoarthritis. *Int J Immunogenet*. 2013;40 (4):272–279. doi:10.1111/iji.12020
48. Ruiz-Miyazawa KW, Pinho-Ribeiro FA, Borghi SM, et al. Hesperidin methylchalcone suppresses experimental gout arthritis in mice by inhibiting NF-κB activation. *J Agric Food Chem*. 2018;66(25):6269–6280. doi:10.1021/acs.jafc.8b00959
49. Zhang T, Wang G, Zheng J, et al. Profile of serum cytokine concentrations in patients with gouty arthritis. *J Int Med Res*. 2021;49(11):1–7. doi:10.1177/03000605211055618
50. Cavalcanti NG, Marques CD, Lins ELTU, et al. Cytokine profile in gout: inflammation driven by IL-6 and IL-18? *Immunol Invest*. 2016;45 (5):383–395. doi:10.3109/08820139.2016.1153651
51. Lopez-Castejon G, Brough D. Understanding the mechanism of IL-1β secretion. *Cytokine Growth Factor Rev*. 2011;22(4):189–195. doi:10.1016/j.cytogfr.2011.10.001

52. Yokose K, Sato S, Asano T, et al. TNF-α potentiates uric acid-induced interleukin-1β (IL-1β) secretion in human neutrophils. *Mod Rheumatol*. 2018;28(3):513–517. doi:10.1080/14397595.2017.1369924
53. Kim KW, Kim BM, Lee KA, et al. Reciprocal interaction between macrophage migration inhibitory factor and interleukin-8 in gout. *Clin Exp Rheumatol*. 2019;37(2):270–278.
54. Schweyer S, Hemmerlein B, Radzun HJ, et al. Continuous recruitment, co-expression of tumour necrosis factor-alpha and matrix metalloproteinases, and apoptosis of macrophages in gout tophi. *Virchows Arch*. 2000;437(5):534–539. doi:10.1007/s004280000282
55. Faust HJ, Zhang H, Han J, et al. IL-17 and immunologically induced senescence regulate response to injury in osteoarthritis. *J Clin Invest*. 2020;130(10):5493–5507. doi:10.1172/JCI134091
56. Liu Y, Zhao Q, Yin Y, et al. Serum levels of IL-17 are elevated in patients with acute gouty arthritis. *Biochem Biophys Res Commun*. 2018;497(3):897–902. doi:10.1016/j.bbrc.2018.02.166
57. Brevi A, Cogrossi LL, Grazia G, et al. Much More Than IL-17A: cytokines of the IL-17 Family Between Microbiota and Cancer. *Front Immunol*. 2020;11:565470. doi:10.3389/fimmu.2020.565470
58. Mcgeachy MJ, Cua DJ, Gaffen SL. The IL-17 family of cytokines in health and disease. *Immunity*. 2019;50(4):892–906. doi:10.1016/j.immuni.2019.03.021
59. Sud V, Abboud A, Tohme S, et al. IL-17A - A regulator in acute inflammation: insights from in vitro, in vivo and in silico studies. *Cytokine*. 2021;139:154344. doi:10.1016/j.cyto.2018.03.030
60. Dai XJ, Tao JH, Fang X, et al. Changes of Treg/Th17 ratio in spleen of acute gouty arthritis rat induced by MSU crystals. *Inflammation*. 2018;41(5):1955–1964. doi:10.1007/s10753-018-0839-y
61. Wang WW, Yu HW, Zhang B, et al. Interleukin-17A up-regulates thymic stromal lymphopoietin production by nasal fibroblasts from patients with allergic rhinitis. *Eur Arch Otorhinolaryngol*. 2021;278(1):127–133. doi:10.1007/s00405-020-06274-3
62. Luo X, Wu J, Wu G. PPARγ activation suppresses the expression of MMP9 by downregulating NF-κB post intracerebral hemorrhage. *Neurosci Lett*. 2021;752:135770. doi:10.1016/j.neulet.2021.135770
63. Shoji S, Hanada K, Takahashi M, et al. The NF-κB regulator IκBβ exhibits different molecular interactivity and phosphorylation status from IκBα in an IKK2-catalysed reaction. *FEBS Lett*. 2020;594(10):1532–1549. doi:10.1002/1873-3468.13752
64. Lin X, Shao T, Huang L, et al. Simiao decoction alleviates gouty arthritis by modulating proinflammatory cytokines and the gut ecosystem. *Front Pharmacol*. 2020;11:955. doi:10.3389/fphar.2020.00955